Low frequency variability of the Agulhas Current region in a numerical model

K. A. du Plessis

Project presented for the degree of Masters of Science
Oceanography Department, University of Cape Town
February 2013

Abstract:

The Agulhas region is known to be of global importance due to its role in the Global Meridional Overturning Circulation (GMOC) and regionally it can influence rainfall patterns and severe weather events. The long-term variability of the Agulhas region was analysed in relation to temperature, sea surface height (SSH) and velocity within the current using output from a regional ocean model. Validation of the model with *in situ* and satellite observed values for the temperature and SSH showed the modelled SSH results to be only marginally different from the satellite observed, while the temperature validation showed the modelled results to be over-estimating temperature across the region. Relatively weak trends existed in temperature and SSH for some parts of the Agulhas Current, most notably the retroflection region.

There were also periods such as the 1960s and 1990s which were anomalously warm whereas the 1950s and 2000s were relatively cool. Analyses of these periods in terms of atmospheric changes throughout the Southern Hemisphere revealed some connections with El Niño – Southern Oscillation (ENSO), the Southern Annular Mode (SAM) and shifts in the wavenumber 3 or 4 pattern in the mid-latitude atmosphere.

Table of Contents:

1. Literature Review:

The South Indian Ocean anti-cyclonic circulation is bordered to the west by the Agulhas Current. This western boundary current flows down the east coast of South Africa and is comprised of water from the South Indian Ocean gyre and recirculated water from within the Agulhas System itself (Lutjeharms, 2006; Stramma and Lutjeharms, 1997). South of South Africa, the current retroflects back into the South Indian Ocean as the Agulhas Return Current (Lutjeharms, 2007). Shedding of Agulhas rings into the South East Atlantic Ocean occur from this retroflection region (Lutjeharms and Van Ballegooyen, 1988). The shedding of these rings is known to be important for the global thermohaline circulation (Olson and Evans, 1986 ; Gordon *et al.* 1992; Beal *et al.*, 2011) as the rings provide an input of the warm saline Agulhas water into the cooler Atlantic Ocean. The Agulhas Retroflection is often associated with the region where the current passes the southern tip of the African continental shelf (Lutjeharms, 2007). The Retroflection consists of a loop of diameter 300 – 400 km (Lutjeharms and Van Ballegooyen, 1988). The Agulhas Return Current forms the northern-most limit of the Southern Ocean, bordering the Subtropical Convergence, before mixing into the South-West Indian Ocean reduces its signal to a negligible amount (Lutjeharms, 2006). The Subtropical Convergence (STC) is considered to be a component of the Subtropical Front (STF) (James *et al.* 2002). The STF is defined by Orsi *et al.* (1995) as the northern limit of the Antarctic Circumpolar Current (ACC) and is the region where the temperature at 100 m depth changes from 12˚C to 10˚C and the salinity moves from 34.6 to 35.0 psu.

The Agulhas Current:

The Agulhas Current is the strongest western boundary current globally (Bryden *et al.*, 2005). While Jacobs and Georgi (1977) estimated the volume flux of the south Agulhas as 125 Sv (a Sv is $10^6 m^3 s^{-1}$) the Agulhas was found by Bryden *et al.* (2005) over their study period to carry between 90 Sv and 121 Sv (average 69.7 Sv) poleward,. This estimate is in general agreement with other studies (Beal *et al.*, 2011; Grundlingh, 1988). Beal *et al.* (2006) notes the Agulhas Current waters

comprise mainly recirculated subtropical gyre waters, as well as Arabian and Red Sea waters, Indonesian through-flow and equatorial Indian Ocean waters (Song *et al.,* 2004). The Agulhas Current is supplied by three sources (Lutjeharms, 2007). Originally, it was thought that the main influx into the Agulhas Current was from a Mozambique Current which flowed through the Mozambique Channel. It was discovered however that the flow in the Mozambique channel is a stream of eddies rather than a current (De Ruijter *et al.,* 2005). The trail of eddies appears to be influenced by Rossby waves over the South Indian Ocean (De Ruijter *et al.*, 2005). These eddies form the foundation of the Agulhas Current which is fully formed at 30˚S (Lutjeharms, 2006). The second input comes from the East Madagascar Current and associated rings south of Madagascar that track westward towards the northern Agulhas Current (Schouten *et al.*, 2002). The eddies from the Mozambique Channel and Madagascar are thought to assist in the formation of Natal Pulses (de Ruijter *et al.,* 1999). Formed in the Natal Bight, a Natal pulse is a deviation of the warm core of the Agulhas Current off-shore, which in turn may influences the spawning of Agulhas rings at the retroflection (Van Leeuwen *et al.*, 2000). The third input is formed from the influx of recycled Southwest Indian Ocean sub-gyre water (Stramma and Lutjeharms, 1997).

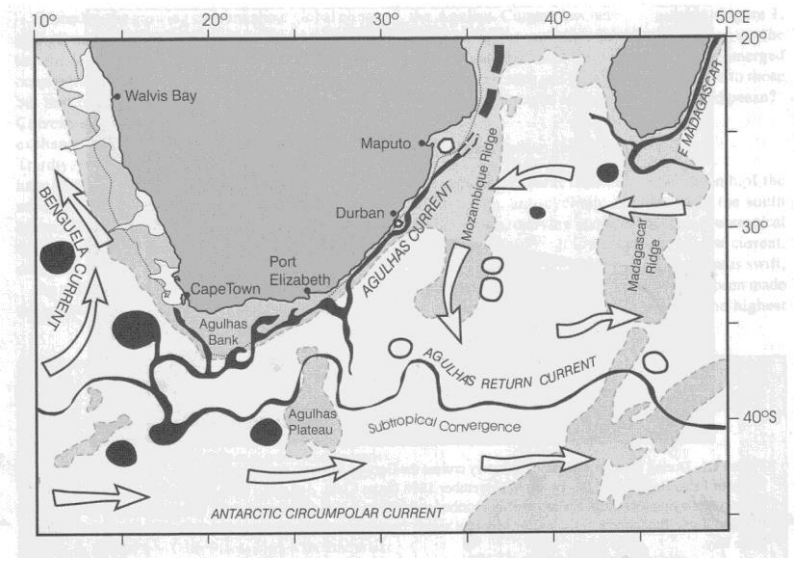

Figure 1.1: Schematic of the Agulhas Current, Retroflection and Return Current. (Lutjeharms, 2006)

The Agulhas Current is divided into the northern and southern Agulhas Current (Lutjeharms, 2006). The northern Agulhas, as noted by Lutjeharms (2006), has an invariant path with the core of the current in close proximity to the shelf edge. This proximity to the steep continental shelf results in stability to the current here (de Ruijter et al., 1999). The exception is the Natal bight, where the current is forced offshore due to the wider shelf. This results in instabilities in the form of Natal pulses, as mentioned above. The southern Agulhas is the section of the Agulhas that flows along the eastern edge of the Agulhas bank, south of Port Elizabeth. The South Agulhas is prone to meanders, as noted by Lutjeharms *et al.* (1989).

The primary driver of the Agulhas Current is thought to be large scale wind patterns over the South Indian Ocean (Lutjeharms, 2006). This is also noted by Beal *et al.* (2011) and Backberg *et al.* (2012) who have stated that a positive wind stress curl over the subtropical South Indian Ocean is responsible for the Agulhas flow. It is found by Le Bars *et al.* (2012) that with an increase in wind stress strength, there is a linear increase of the volume transport of the Agulhas Current. The seasonality of the monsoonal wind regime is thought to have little to no impact on the anti-cyclonic gyre of the South Indian Ocean (Ramage, 1984 from Lutjeharms, 2006) with there being evidence to suggest that the South Indian Ocean is removed from the North Indian Ocean's seasonality. Lutjeharms (2006) notes the contrast between the North Indian and the South Indian Oceans: the South Indian Ocean has a much greater resemblance to other subtropical ocean basins. The Agulhas Current has been found to have a poleward velocity of 1.3 $m.s^{-1}$ ($\pm$ 0.3 $m.s^{-1}$) over the full depth of the current (Grundlingh, 1980).

The Agulhas Retroflection:

The Agulhas Retroflection is located at the termination of the southern Agulhas Current – the current overshoots the continental shelf south of South Africa as a free inertial jet (Lutjeharms *et al.*, 1996), whereupon it turns back on itself. The retroflection is thought to be a result of the principle of conservation of potential

vorticity (Lutjeharms and Van Ballegooyen, 1988) with the loss of the stabilizing continental shelf to the west. However, Lutjeharms and van Ballegooyen (1984) and De Ruijter (1982) suggest that the position of the retroflection is dependent on the volume of the current as well as on the wind stress curl south of South Africa. On average, the retroflection is located between 16˚E and 20˚E, with an average diameter of 340 km (Lutjeharms and van Ballegooyen, 1988). The retroflection has been found to be extremely important to the Atlantic Meriodional Overturning Circulation (AMOC) (Olson and Evans, 1986), through the spawning of Agulhas rings. As mentioned above, instabilities in the current result in meanders which, upon their arrival at the retroflection, cause a ring of warm saline water to become "pinched off" from the main current (Boudra and de Ruijter 1986). These rings meander westward into the South Atlantic where they provide an important input of heat and salt into the basin (Gordon *et al.,* 1992). The so called "Agulhas leakage" of these rings has been found to be connected with the termination of glacial periods – Beal *et al.* (2011) suggested that with an increase in leakage into the South Atlantic, there was rapid deglaciation. The intensity of the leakage is reliant on the position of the STC: with a southward shift in the STC, Beal *et al.* (2011) suggests that there is an increase in leakage into the South Atlantic, and vice versa with a northward shift in the STC. However, Beal *et al.* (2011) also notes that the Agulhas leakage is a complex interaction of mechanisms, with the strength of the Agulhas Current playing a role. It is thought that with the increase in strength of the current, there would be a decrease in the leakage if the wind pattern remained constant. Le Bars *et al.* (2012) shows that at high wind stress magnitudes a turbulent regime appears, causing a plateau of the volume leaking into the Atlantic. With the current changes in global winds, research suggests a southward expansion of the wind pattern: the effect this may have on the intensity of the leakage is largely unknown (Beal *et al.*, 2011; Le Bars *et al.*, 2012).

The Agulhas Return Current:

The Agulhas Return Current is the remaining flow after the spawning of Agulhas rings

at the retroflection, and is defined by Lutjeharms and Ansorge (2001) as a continuing link of the South Atlantic Current into the South Indian Ocean Current. Lutjeharms and van Ballegooyen (1988) found the Agulhas Current retroflects almost in its entirety and flows parallel to the STC. This region is found to have the steepest thermal gradients globally (Lutjeharms, 2006) due to the close proximity of the warm Agulhas Return Current to the northern boundary of the cool Southern Ocean within the Subtropical Front. The warm Return Current is about 90km wide (Lutjeharms and van Ballegooyen, 1988) and is defined by large meridional meanders, noted by Lutjeharms (2006) to be a result of the steep meridional thermal gradient of the current. These meanders are found by Lutjeharms and van Ballegooyen (1984) and Grundlingh (1978) to be around 27˚E and 32˚E. Due to the strong heat exchange associated with the warm surface water and the cool overlying air, the character of the Return Current is rapidly altered downstream (Lutjeharms, 2006). Lutjeharms and Ansorge (2001) found that the current lies at a latitude of 39˚30' S, however it shifts southward downstream to 44˚30'S at 60˚E. Lutjeharms and Ansorge (2001) noted that the Return Current interacts with the local bathymetry, resulting in northward meanders in the current of up to 2˚30'. The current is thought to be zonally continuous, with its termination lying between 66˚E and 70˚E (Lutjeharms and Ansorge, 2001).

The Subtropical Front:

The Subtropical Front (STF) is defined by Orsi *et al.* (1995) as the northern boundary of the Antarctic Circumpolar Current (ACC) and as the boundary between the subtropical waters associated with the Agulhas Return Current and the sub-Antarctic waters (Lutjeharms and Valentine, 1984; Lutjeharms *et al.* 1985). Orsi *et al.* (1995) define the position of the STF as the latitude where the temperature changes from 12˚ to 10˚ at 100 m, and the salinity changes from 34.6 psu to 35.0 psu at 100 m. The mean position of the STF south of South Africa is found by Lutjeharms (1984) to be 42˚S. Recent studies show that the STF may be an intermittent feature that is strengthened by the Agulhas Return Current (Burls and Reason, 2006; James *et al.*,

2002), contrasting with earlier research that suggests that the STF is a feature that exists continuously across the South Atlantic (Orsi *et al.*, 1995). Billany *et al.* (2010) showed that using Mean Absolute Dynamic Topography (MADT), the fronts in the Southern Ocean (including the STC) can be located, consistent with the position of the front hydrographically. The steep gradient associated with the STF can therefore be used to locate it. The STF is seen by Belkin and Gordon (1996) as having both a north and southern branch. The southern STF is traditionally considered the STC, with a seasonal migration of 2.5˚ latitude (Burls and Reason, 2006). These shifts are associated with the changes in the wind fields and the wind stress curl (Cai *et al.*, 2005). James *et al.* (2002) notes that the position of the STC is characterized by the negative wind stress curl and therefore Ekman transport convergence.

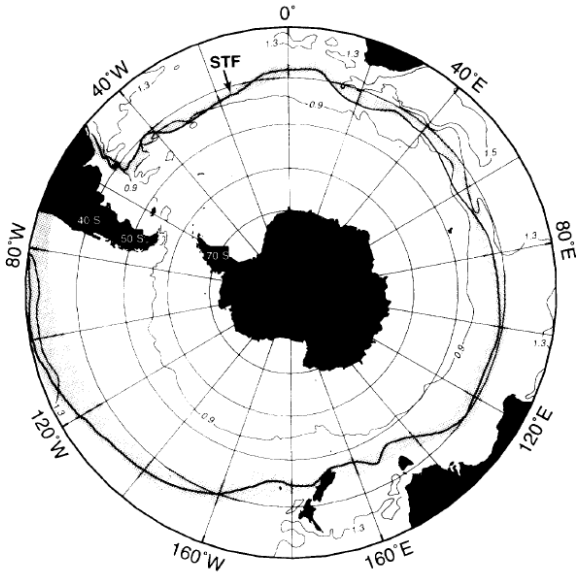

Figure 1.2: Position of the Subtropical Front (STF) from a polar view (Orsi *et al.*, 1995).

Seasonal Variability of the Region:

The seasonal variability of the Agulhas region is associated with wind patterns over the South Indian Ocean (Beal *et al.*, 2011). It is noted that with a shift in these wind fields there may in turn be a change in the Agulhas Current, as well as changes in the retroflection, leakage into the South Atlantic, and the Return Current (Beal *et al.,*2011; Backeberg *et al.*, 2012). The wind patterns associated with the STC are

considered to be the westerly winds that drive the Antarctic Circumpolar Current (Orsi *et al.,* 1995). Alteration of these wind fields may cause a southward or northward shift in the STC, impacting on the Agulhas retroflection and the leakage into the Atlantic (Beal *et al.*, 2011). With an increase in the Southern Ocean wind field intensity, a northward shift of the STC would cause a decrease in the leakage into the South Atlantic, which in turn would affect the AMOC (Beal *et al.*, 2011).

Interannual Variability:

The El Nino – Southern Oscillation (ENSO):

El Nino and La Nina are key drivers of interannual variability within the Pacific Ocean, however their influence is felt globally (Reason *et al.*, 2000). An El Nino event is associated with a reduction in the trade winds over the Pacific and a pooling of warm water off the west coast of South America, while a La Nina event is associated with stronger trade winds and an intensification of cool, upwelled waters off the west coast of South America (Trenberth, 1997). Colberg *et al.* (2004) find that there is a coherent response to both El Nino and La Nina events in the South Atlantic. The response to ENSO in the South Atlantic is found by Colberg *et al.* (2004) to have a season's delay, and is evident in a change in the sub-surface temperatures (temperatures in the mid-latitudes decrease) and a weakening in the subtropical anti-cyclonic gyre across the basin. Similarly Reason *et al.* (2000) show that the climate variability over the Indian Ocean responds to El Nino and La Nina with about one season lag behind the SST and wind changes in the tropical Pacific. Reason *et al.* (2000) show that the change seen in sea surface temperature (SST) is attributed to changes in cloud cover and wind strength over the Indian Ocean as a result of the El Nino/La Nina event. These remote wind and cloud cover changes may occur through atmospheric Rossby and Kelvin wave propagation from the tropical Pacific forming an atmospheric bridge – a type of teleconnection that results in ENSO impacting globally (Alexander *et al.* 2002). Alexander *et al.* (2002) note that there is a clear link between SST anomalies in the Pacific and SST anomalies in the Atlantic and Indian oceans. The key link to the atmospheric bridge is the ocean heat flux (Alexander *et*

al., 2002). Warmer SST and subsurface temperatures occupy the western central Indian Ocean during El Nino (Reason *et al.,* 2000; Tourre and White, 2005). Tourre and White (2005) find that variance associated with the ENSO signal has a similar in the Indian Ocean to that in the Pacific Ocean, however the underlying forcing has a different origin.

Beal *et al.* (2011) observed that the paleontological coral records show the influence of climate variability on the Agulhas region. The increase in temperatures in the Agulhas region since the 1970s may result in an increased sensitivity to the African hydrological cycle, as ENSO affects African rainfall events (Reason and Rouault, 2002; Beal *et al.* 2011). El Nino is described as weakening the Indian Ocean subtropical gyre, as well as causing a latitudinal shift in the ocean patterns (Beal *et al.*, 2011). The opposite is associated with La Nina – a strengthening of the gyre. These alterations within the subtropical gyre in turn affect the source of the Agulhas Current and ultimately the Agulhas leakage (Schouten *et al.*, 2002; Beal *et al.*, 2011).

The Southern Annular Mode:

The main driver of the changes in the wind fields over the Southern Hemisphere has been attributed to the Southern Annular Mode (SAM) (Marshall, 2003), also referred to as the Antarctic Oscillation (Carlton, 2003; Jacobs, 2006). The SAM has been shown to be the leading mode of climate variability in the Southern Hemisphere south of 20^{o}S (Lenton and Matear, 2007). The SAM is defined by Marshall (2003) as the difference between mean sea level pressure anomalies observed at six surface stations close to 40˚S and another six close to 60˚S. Alternatively, the SAM can be defined as "the time series of the first Empirical Orthogonal Function (EOF) of the 850 hPa geopotential height anomaly" (Lenton and Matear, 2007). The SAM has been shown to influence rainfall in western South Africa (Reason and Rouault, 2005) and midlatitude South America (Silvestri and Vera, 2003), as well as have an effect on the wind stress curl (Cai *et al.*, 2005). However Billany *et al.* (2010) showed that there does not appear to be a strong correlation between the SAM and position of

the fronts at the Greeenwich Meridian over seasonal to interannual time scales.

Jacobs (2006) has noted that there is an upward trend in the SAM, with a maximum change in wind stress curl at approximately 48˚S (Cai *et al.*, 2005). Gillett *et al.* (2006) observed that outside of Antarctica, there is a significant increase in ocean temperature associated with a positive SAM in the 40˚S to 60˚S latitude, however north of 40˚S, there is not an evident temperature response. Hall and Visbeck (2002) noted that with a positive SAM there is a strengthening of surface westerlies at around 55˚S and a weakening of the westerlies at around 35˚S. This is in agreement with research by Hartman and Lo (1998), Limpasuvan and Hartman (1999) and Lovenduski and Gruber (2005). The effect of the SAM on the Southern Ocean is seen in the influence of the SAM on air-sea fluxes, with the positive trend in the SAM resulting in a decrease in Southern Ocean carbon dioxide uptake (Lenton and Matear, 2007), along with affecting the wind stress curl mentioned above.

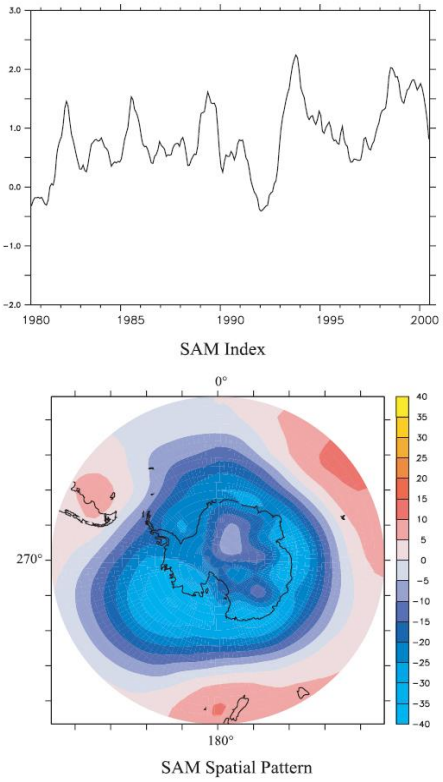

Figure 1.3: Variability and spatial representation of the SAM (Lenton and Matear, 2007)

2. Introduction:

The subtropical South Indian Ocean is characterized by warm, saline water and is linked to global circulation through its western boundary current, the Agulhas Current. The Indian Ocean has two circulation regimes: the North Indian Ocean circulation is dominated by the monsoon-controlled North Indian gyre and the South Indian Ocean circulation is an anticlockwise, basin-wide gyre, independent of the northern monsoon system (Lutjeharms, 2006). Inflow into the southern gyre occurs through the Indonesian through-flow that flows south of the equator (Lutjeharms, 2006). At the western boundary of the gyre, flow is southward along the east coast of South Africa in the form of the Agulhas Current. The Agulhas Current turns back on itself at the Agulhas retroflection, where between 2 Sv and 15 Sv flow from the Indian Ocean into the South Atlantic through Agulhas rings at the leakage (Beal *et al.* 2011), with the rest returning into the Indian Ocean through the Agulhas Return Current (Lutjeharms and Ansorge, 2001). The Agulhas Return Current carries this remaining Indian Ocean water eastward, along the Subtropical Front (STF) (Lutjeharms, 2006).

The Agulhas region is of importance due to its role in global ocean circulation and the global climate (Biastoch *et al.,* 2009; Beal *et al.* 2010). Variability within the Agulhas region may result from changes in the wind fields (de Ruitjer *et al.* 1999, Beal *et al.* 2011, Le Bars *et al.* 2012) which alter the velocity of the current and thus the sea surface temperature (SST) and the sea surface height (Billany *et al.* 2010, Backeberg *et al.*, 2012). Improved understanding of low frequency variability of the Agulhas Current system is required to assess the role that this current plays in regional and global climate. Large scale climate modes such as the El Nino Southern Oscillation (ENSO) and the Southern Annular Mode (SAM) are suspected to have an influence on the ocean and atmospheric variability seen south of Africa (Colberg *et al.*, 2004; Lovenduski and Gruber, 2005) and thus in turn may have an influence upon the Agulhas region. The extent of this influence however has not been explored in detail.

As the western boundary current of the South Indian gyre, the Agulhas is a fast flowing (Bryden *et al.* (2005) calculate an average of 70 Sv) warm ribbon of water that is divided into a northern and southern section (Lutjeharms, 2006) The current is driven by a positive wind stress curl over the South Indian Ocean (Lutjeharms, 2006). Rouault *et al.* (2009) observed a warming trend in the Agulhas system since the 1960s, which they attributed to increased wind stress curl.

Anomalies in the wind stress curl over the South Indian Ocean may change the transport of the current and thus the sea surface height (SSH) (Billany et al., 2010). Inflow into the northern Agulhas Current is from three sources: flow from the Mozambique Channel, flow from the East Madagascar Current and recirculation in the South West Indian Ocean (Lutjeharms, 2006).

The temperature of the upper ocean in the Agulhas Current region is affected by external forcing such as ENSO (Reason *et al.* 2000; Rouault *et al.*, 2010) through atmospheric tele-connections, local surface forcing and altered inflow into the source of the current (De Ruijter *et al.*, 2005). However the extent of this influence of ENSO on the Agulhas region is not fully understood. Both El Nino and La Nina events affect upper ocean temperature, with Rouault *et al.* (2010) noting that the SST on the east coast of South Africa has, in general, a negative correlation to ENSO. Reason *et al.* (2006) attribute part of the variability within the region to variability in the tropical Indian Ocean, along with atmospheric bridging changing the wind stress curl and thus influencing the strength of the current.

El Nino events generally lead to a weakening in the South Indian Ocean trade winds which can alter the forcing of the Agulhas Current (Harrison and Larkin, 1998). Quantifying this relationship between ocean temperatures, SSH and ENSO is of importance in that changes in sea surface temperatures across the Agulhas region are found by Reason and Mulenga (1999) and Reason and Rouault (2002) to impact on the seasonal rainfall of southern Africa. Given these relationships between SST in

the Agulhas region and seasonal rainfall, it is important to establish an understanding of ENSO correlations with ocean temperatures within the region.

Both the ENSO and the SAM cause large scale changes in surface winds which can then alter the Agulhas Current through their effect on the wind stress curl. SAM, the dominant mode of climate variability in the mid- and high latitude Southern Hemisphere (Marshall, 2003), directly impacts wind stress curl over the mid-latitude Southern Hemisphere. A strong positive SAM event is characterised by an increase in the intensity of the westerly winds in the latitudes around 60˚S and a decrease in intensity of the westerly winds around 40˚S, giving an increased gradient of wind stress across the region.

The SAM is predicted by climate models (Cai *et al.*, 2005) to have an upward trend in the future, which could strengthen the Southern Ocean super gyre and modify ocean fronts with the shifting wind regimes in the Southern Ocean (Jacobs, 2006; Hall and Visbeck, 2002). This is significant for the Agulhas region as a shift of the Subtropical Front (STF) is found by Biastoch *et al.* (2009) and Beal *et al.* (2011) to alter flow into the Atlantic at the Agulhas retroflection. However the extent of the connection between the SAM and flow through the Agulhas retroflection has yet to be fully explained. This change in leakage into the South Atlantic is dependent on both the intensity of the flow in the Agulhas Current and the position of the Subtropical Front (STF) to the south of the retroflection (Beal *et al.,* 2011).

A northward shift in the STF is found to reduce the leakage into the South Atlantic and conversely a southward shift in the STF is associated with an increased leakage (Biastoch *et al.* 2009; Beal *et al.* 2011). The influence of the SAM on the Agulhas is of global significance through the effects on the Agulhas leakage. An increase in the leakage could result in a strengthening of the thermohaline circulation in the Atlantic (Beal *et al.,* 2011), with the rate of leakage into the Atlantic related to global climate change. Variability within the Agulhas region alters leakage into the South Atlantic,

impacting on the thermohaline circulation (Biastoch *et al.*, 2009; Beal *et al.*, 2011). Biastoch *et al.* (2009) note that while changes in the Agulhas region impact the circulation, these influences have not been fully resolved and quantified.

The average position of the Agulhas retroflection is 42˚S (Orsi *et al.,* 1995), however Lutjharms and Van Ballegooyen (1984) have proposed that the Agulhas Retroflection position shifts in response to the intensity of the flow within the current. With an increase in flow within the current there is a westward shift in the retroflection (Beal *et al.*, 2011). This shift continues until instability causes a budding-off of an Agulhas ring (Lutjeharms, 2006). These rings propagate into the South Atlantic, providing the integral connection to the global thermohaline circulation through the input of saline, warm water (de Ruijter *et al.,* 2005) and therefore transferring energy (Olsen and Evans, 1986) from the Indian Ocean to the cooler South Atlantic Ocean. While the SAM affects the wind regimes of the Southern Hemisphere (Lovenduski and Gruber, 2005), and the wind regimes are found to alter the retroflection and the Agulhas Current as a whole (Beal *et al.*, 2011; Biastoch *et al.,* 2009), there has been little investigation into a direct link between the SAM and the Agulhas region.

The Subtropical Front (STF) is the southern-most limit of the warm Agulhas return water and marks the boundary of the Southern Ocean and the Indian Ocean (Lutjeharms and Valentine, 1984). The STF is characterized by a steep temperature gradient (Orsi *et al.* 1995), as well as being a region of intense velocity, which in turn results in a noticeable change in Sea Surface Height (SSH) (Backeberg *et al.,* 2012). Billany *et al.* (2010) note that the position of the STF can be located using the changes in the meridional gradients of SSH. Some of the variability in the STF might be attributed to changes in the wind patterns over the Southern Ocean (Burls and Reason, 2006). An increase in the intensity of the winds is found to cause a northward shift in the STF, while a decrease in wind strength causes a southward shift in the STF (Beal *et al.*, 2011). These shifts in the STF alter the Agulhas leakage by narrowing the area available for the retroflection loop and thus altering flow into the

Atlantic (Beal *et al.* 2011). Variability in the position of the STF would denote a change in the flow of the region along the front, and possibly therefore a lower transport along the STF.

Rasmusson and Carpenter (1982) find that changes in temperature (principally SST) are connected to the surface winds. In turn surface winds are found by Ekman (1905) to be the drivers of transport in the ocean, therefore changes in the surface wind in turn alters the transport within the water column (Ekman, 1905; Price *et al.*, 1987). The change of transport and mixing caused by the surface wind is displayed in the change in the SST (Rasmusson and Carpenter, 1982). Similarly, the SST is found by Namais (1973) (found in Wallace *et al.,* 1992) to be positively correlated with sea level pressure (SLP) and geopotential height (GPH). Rogers and van Loon (1982) find that mid-latitude anomalies of SLP and 500 mb GPH are of opposite signs to those over Antarctica. They further conclude that these differences are used to explain the zonal winds associated with the region, as well as the connection between the zonal winds and the SAM.

The SLP and GPH are shown by Carleton (2003) to form into set wave patterns, with a wavenumber representing the number of peaks contained within the atmospheric circulation pattern. Carleton (2003) notes that a wave-number 2, with an intense interannual variation of the low pressure found above the Amundsen Sea, is associated with an ENSO signal. Similarly, Carleton (2003) suggests that the Antarctic Oscillation (otherwise known as SAM – Marshall, 2003) is associated with a zonally symmetrical atmospheric pattern. Thus the SLP and GPH across the Southern Hemisphere are useful in the identifying of large scale planetary waves in the atmosphere which in turn are associated with global climate patterns such as the SAM (Rogers and van Loon, 1982). Therefore these patterns may be helpful in identifying forcings of variations within the Agulhas region.

Given the importance of variability in the Agulhas Current region for climate and the relative lack of understanding in how large scale climate modes may influence the current, this thesis addresses the following research questions:

1. What are the low frequency variability patterns in temperature, sea surface height and velocity within the Agulhas region? Do any statistically significant trends exist?

2. What is the strength of the correlation between temperature/sea surface height in the Agulhas Current region and ENSO and SAM?

3. What are the potential mechanisms associated with the low frequency variability in the current?

3. Methods:

Monitoring of variability within the Agulhas region is of global importance, as the region significantly affects thermohaline circulation (Beal *et al*. 2011). The change in variability of the region impacts on the inflow of warm saline water into the South Atlantic, through the Agulhas retroflection and leakage. The analysis of long term variability within the Agulhas region requires a length of data record that includes interannual and decadal variability. This is only possible through the use of ocean models, as ocean models provide a realistic continuous output.

Model Overview:

The Regional Ocean Modelling System (ROMS) is a split-explicit, free-surface model that is solely for oceanic variables, and is defined into topographically-following curvilinear co-ordinates. Schchepetin & McWilliams (1998) note that ROMS includes time-step algorithms with both forward and backward feedback, as well as barotropic mode equations that decrease mode-splitting error through accounting for non-uniform density fields. Dispersion within the model is limited, and steep pressure gradients are preserved through a third-order upstream biased advection scheme, along with other higher order numerics (Shchepetkin and McWilliams, 1998).

ROMS is used here as the AGIO model configuration, a domain subset of ROMSTOOLS (Penven et al., 2008). AGIO has a resolution of 1/4˚, with a Mercator grid extending from 29˚W to 115˚E and from 7˚N to 48.25˚S. This results in a mean grid spacing of 23km over the Agulhas region. Regional bathymetry derived from GEBCO, is smoothed to decrease pressure gradient errors, through a selective filter keeping the slope parameter R equal to 0.2 (Haidvogel & Beckmann, 1999). The vertical resolution of the model is defined by 32 layers that are altered by bathymetry, and stretched towards the surface in accordance with Haidvogel & Beckmann's (1999) methods. The lateral viscosity in the interior of the model is zero however this increases towards the domain perimeter. An active radiation scheme

(Marchesiello *et al.*, 2001) links external variables to the internal, analytical variables. Within the boundary layer, topographic interactions are determined by a bottom-drag quadratic equation and KPP parameterization. Bottom topography is smoothed towards external bathymetry to limit discontinuity at the boundary. The boundary conditions for the experiment are derived from global ORCA05 model configurations, described by Durgadoo *et al.* (2013 about to be submitted). Similarly, reanalysis products from CORE v.2b, normal year and 1948 to 2007 interannual, are used at the surface to force simulations (Large & Yeager, 2004; Large and Yeager, 2009).

Five day averages of a subsection of the model domain were extracted, for the time period 1948 to 2007, over the region 22˚S to 44˚S and 10˚E to 45˚E. Within this, the current was divided into a further five blocks. The variables studied were averaged within these blocks, similar to the method used by Backeberg *et al.* (2012). The latitude of these sections can be seen in Table 1. The most northerly section covers the inflow into the northern Agulhas Current, each consecutive block progressively further south-west, with the fourth block over the Agulhas retroflection region. The fifth block covers the Agulhas Return Current and the Subtropical Front (STF).

Table 3.1: Position of the analysed blocks within the study region

Block	Latitude (˚S)	Longitude (˚E)
Northern Agulhas Current	26 – 29	33 – 40
Central Agulhas Current	29 – 32	30 – 33
Southern Agulhas Current	33 – 36	24 – 28
Agulhas Retroflection Region	36 – 42	16 – 20
Agulhas Return Current & STF	40 – 44	20 - 42

Model Validation:

The validation of the model output was performed for temperature (at 150 m), sea surface temperature (SST) and sea surface height (SSH) through comparison with observational data. The all the variables used within the validation were analysed

over the entire Agulhas region (22˚S to 44˚S and 10˚E to 45˚E). The data for comparison with temperature and SST was extracted from the World Ocean Atlas (09) (WOA09) database, for the years 1948 to 2007. The WOA09 data is taken from all available temperature profiles from 1772 to 2008, however the Agulhas region, inside the Southern Hemisphere is within the region were the WOA09 data was calculated into five climatologies (1955 to 1965, 1965 to 1974, 1975 to 1984, 1985 to 1994, 1995 to 2006) from the total data set. This was then averaged into a mean climatology, with the region of greatest accuracy from 1955 to 2006, similar to the time series it was compared with (1948 to 2007).

The SSH calculated by the model was compared with AVISO Maps of Absolute Dynamic Topography (MADT). The MADT is a gridded product taken from Ssalto/*Duacs* multimission altimeters (taken from Jason-1 and 2, T/P, Envisat, GFO, ERS-1 and 2, and Geosat satellites). The AVISO data is a mean of daily MADT over ten year (1997 to 2007), providing an accurate short term record of MADT over the Agulhas region. This was compared against the modelled results.

Variables Analysed:

The variables considered are sub-surface temperature, across a depth of 150 to 200 metres, sea surface height and meridional velocity. Sub-surface temperatures have more freedom to vary since, unlike the surface temperature, they are not tightly constrained to the imposed atmospheric forcing. Sea surface height (SSH) is considered to be related to velocity within the surface layer, which in turn is related to atmospheric variations, thus useful in exploring the long term trends of the region. Billany *et al*. (2010) notes that the analysis of SSH gradients allows for the determining of the position of fronts within the Southern Ocean, thus through SSH the position of the Subtropical Front (STF) may be determined. Variability within SSH is similarly related to changes in global atmospheric influences such as El Nino and SAM.

Climate Explorer Data:

El Nino and Southern Annular Mode (SAM) indices used within the study were extracted from Climate Explorer, a web-based application used to statistically analyse climate data (http://climexp.knmi.nl).

The El Nino index extracted from Climate Explorer is NINO3.4, and is sourced from KAPLAN NINO34 reconstructed indices for the first two years of the time series (1948 to 1949), after which the index is extracted from the NOAA Climate Prediction Centre Reynolds OI SST for the remainder of the time series (1950 to 2007). SAM indices are drawn from the British Antarctic Survey (BAS) with the index calculated in the same manner as that reported by Marshall (2003).

Computing:

Extracted data from ROMS was analysed through MATLAB, in conjunction with functions within ROMSTOOLS (Penven *et al.*, 2008). MATLAB is a computing program that graphs and plots data, and is useful for the analysis of large data files. MATLAB is capable of performing various numerical analyses including linear analysis, analysis of multiple variables, input data analysis and modelling.

The anomalous temperature and SSH, along with meridional (for the Northern, Central and Southern Agulhas blocks) and zonal (for the STF block) velocity were plotted for the time series with the data standardized

x = (y-mean of y)/std dev

where x is plotted result and y is modelled data. The data then had a 7 year running mean applied, to smooth out the high variability. This moving average filter was performed using the MATLAB.

Correlations performed between modelled data and ENSO and SAM indexes were

calculated through the MATLAB function 'corrcoef'. The function calculates the correlation between the data and the ENSO or SAM index with the equation:

C(i,j)/SQRT(C(i,i)*C(j,j)).

Where C is the covariance matrix, and "i" and "j" are the elements of comparison, ENSO or SAM and sub-surface temperature or sea surface height (SSH). The output of the correlation is in the form of "R" and "P" values. The R value for the correlation displays the correlation between the data - the significant results being found close to 1 or -1. Correlation values that are not higher than 0.3 or lower than -0.3 are not considered to be strong. The P value calculated displays the depth of significance of the data, with a high P value (close to 1) suggesting a high chance of co-incidental correlation, while, a low P value (less than 0.05) shows that the probability that correlation could occur coincidentally is less that 5%, and is therefore statistically significant.

Wavelet analysis of the temperature and SSH time series extracted from the dataset was performed through the Climate Explorer interface. Wavelet analysis indicates how relative peaks in the frequency of signals may vary in strength through the record.

Analysis of Periods of Relatively Large Anomalies:

The differences in four periods of heightened anomalies (periods where the anomalies could be seen to be greatly removed from the mean) were analysed in detail using anomalous SST, sea level pressure (SLP), geopotential height (GPH) and zonal wind speed. These differences between the periods of heightened anomalies were plotted using the http://www.esrl.noaa.gov website over the Southern Hemisphere, for the time periods of interest: 1960 to 1968 against 1950 to 1956, and 1990 to 1996 against 2000 to 2006. The SST data is from the NOAA Extended Reconstructed SST (ERSST V3) data set (Smith *et al.,* 2008; Xue *et al.*, 2003). The

NOAA Reconstructed SST data set is comprised of the International Comprehensive Ocean-Atmosphere Data Set (ICOADS), along with statistical models that have reconstructed data, such that the data set begins in 1854. Thus the time periods of heightened anomalies (1950 to 1956, 1960 to 1968, 1990 to 1996 and 2000 to 2006) are covered easily by the NOAA data set.

The SLP data are extracted from the NCEP/NCAR Reanalysis data set (Kalnay *et al.,* 1996) for the selected periods of heightened anomalies. The NCEP/NCAR Reanalysis project is a data assimilation program, through the website www.esrl.noaa.gov that uses data from 1948 to the present. Similarly the GPH data is taken from the NCEP/NCAR Reanalysis data set (Kalnay *et al.*, 1996) at 500mb as this is the pressure level at which large scale teleconnection patterns associated with ENSO are clearly evident (e.g. Rogers and van Loon (1982). The surface zonal wind differences were extracted from the same data set for the periods of strong anomalies, to give an indication of potential changes in Ekman transport and upper ocean mixing which may then impact on SST.

4. Validation:

As the modelled data is calculated through the use of equations, validation with *in situ* data is required to establish the accuracy of the model's representation of the region. Temperature validations at 150 m, performed using World Ocean Atlas (WOA) data as the *in situ* data show the modelled data to be generally warmer across the region than the WOA data (Figure 4.1). The modelled data represented on the right shows a warmer current and more noticeable, in the bottom image of Figure 4.1, is the difference in the retroflection, where the modelled data is thought to be close to 4 degrees warmer than WOA data. Similarly Figure 4.2, showing the variation on SST between WOA and modelled data, shows a difference of around 4 degrees in the South Agulhas. The modelled SST south of the STF is also warmer than the WOA data.

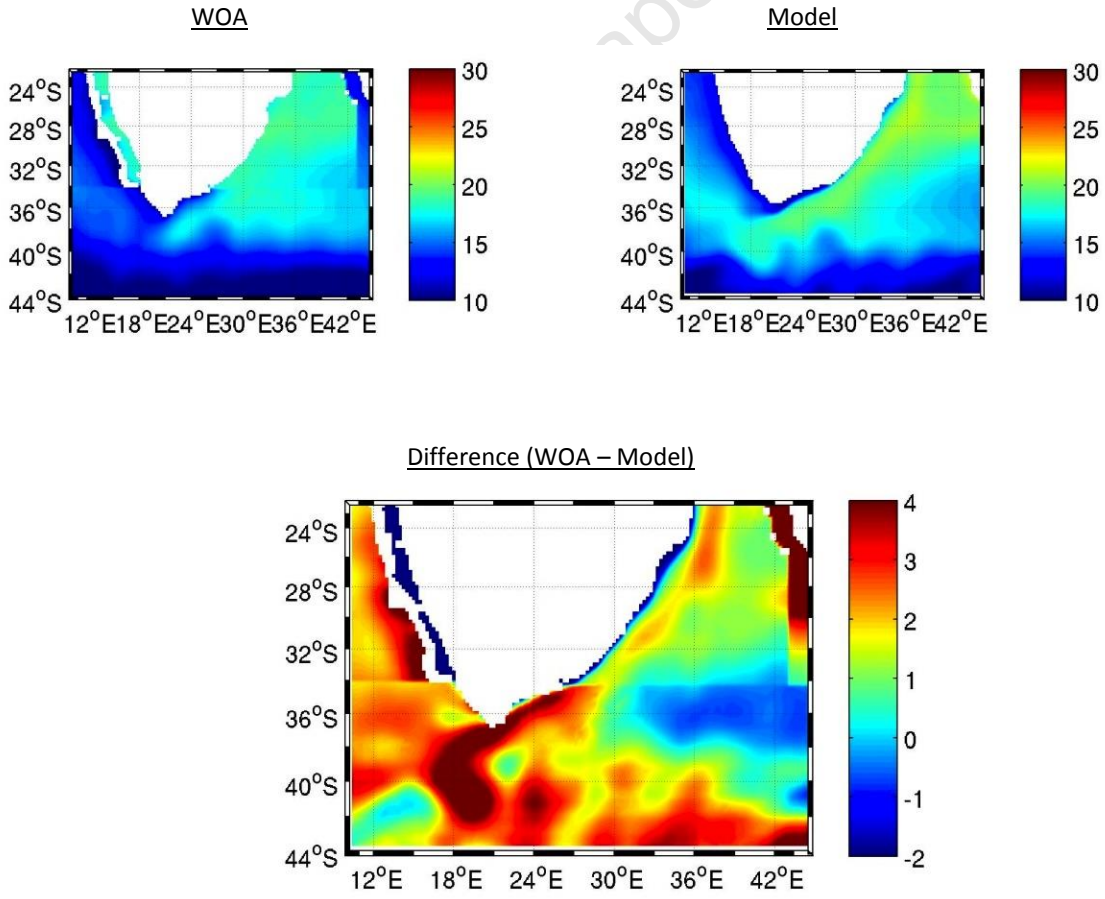

Figure 4.1: Validation of temperature at 150m with World Ocean Atlas data

This over-estimation of both the temperature at depth and the SST will result in a distortion of results in areas with heightened differences. These regions' disparities will not be normalized by the subtraction of the mean, and therefore areas such as the retroflection and the region to the south of the STF may return higher temperatures. However this difference between the modelled data and WOA is thought to be constant, and therefore have little effect on the trends explored in this study.

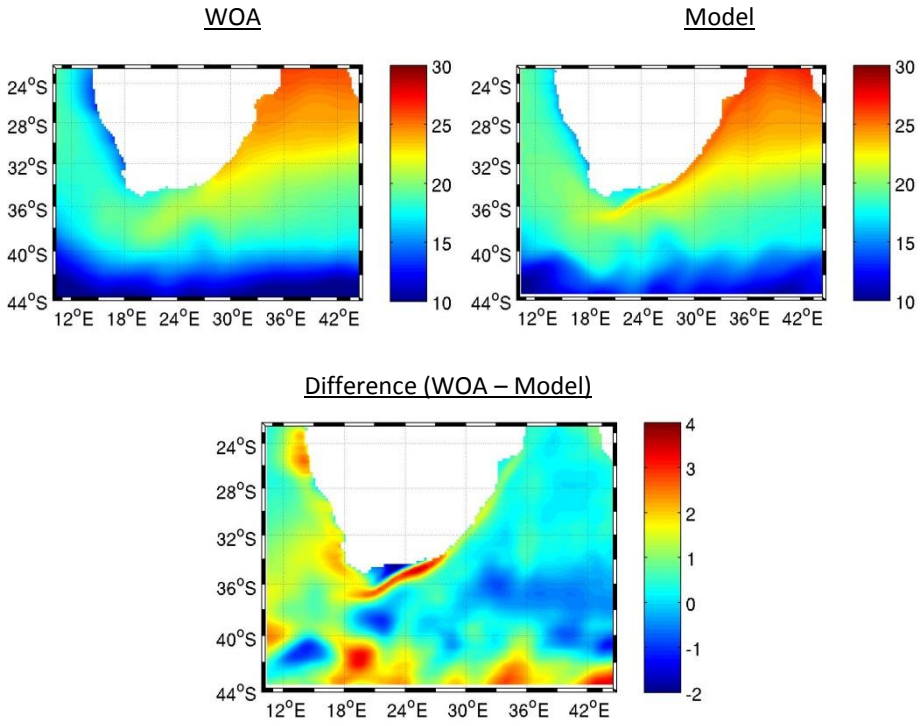

Figure 4.2: Validation of Sea Surface Temperature with World Ocean Atlas data

The SSH validation of the modelled data against AVISO Mean Dynamic Topography (MDT) is seen in Figure 4.3. The SSH validation shows the modelled data to be under-estimating SSH, with SSH in the AVISO data being higher over the Agulhas region. However the modelled data has a higher SSH in the retroflection loop (Figure 4.3). The model calculation of a lower SSH across the Agulhas region is minimal and with the subtraction of the mean for further analysis this discrepancy will be removed. However the intense variation of SSH within the Agulhas Retroflection may result in an inconsistency over that area.

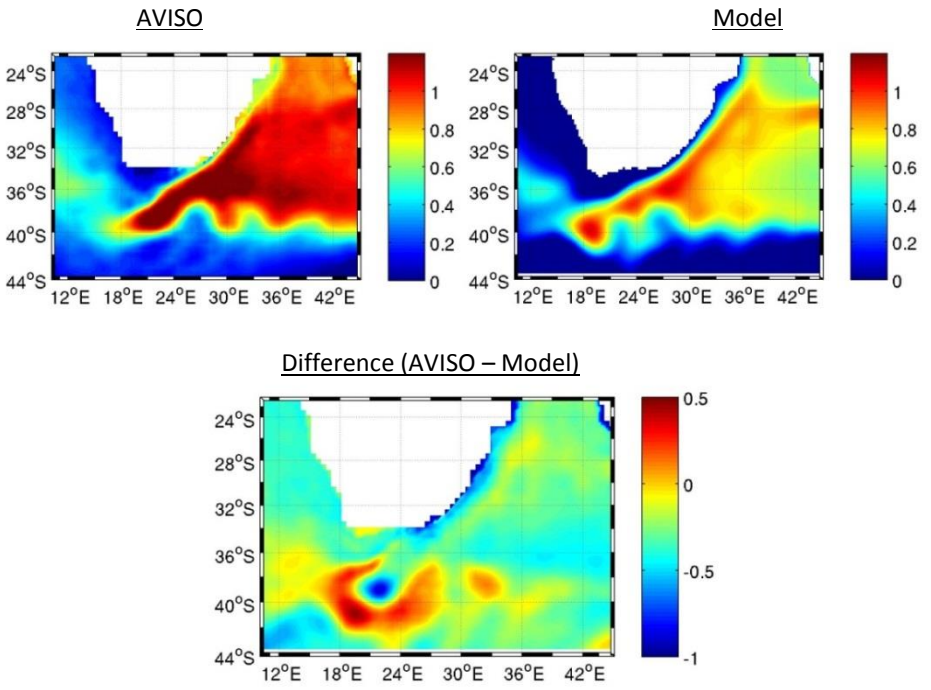

Figure 4.3: Validation of SSH with AVISO Mean Dynamic Topography

5. Results:

Long term variability within the Agulhas region for the time series 1948 to 2007 was analysed through temperature, sea surface height (SSH) and velocity for the five regions (Figure 5.1). The most northerly block accounts for the Northern Agulhas, the second block moving southward for the central Agulhas, the next for the South Agulhas, then the Agulhas Retroflection and the most southerly block for the Subtropical Front (STF).

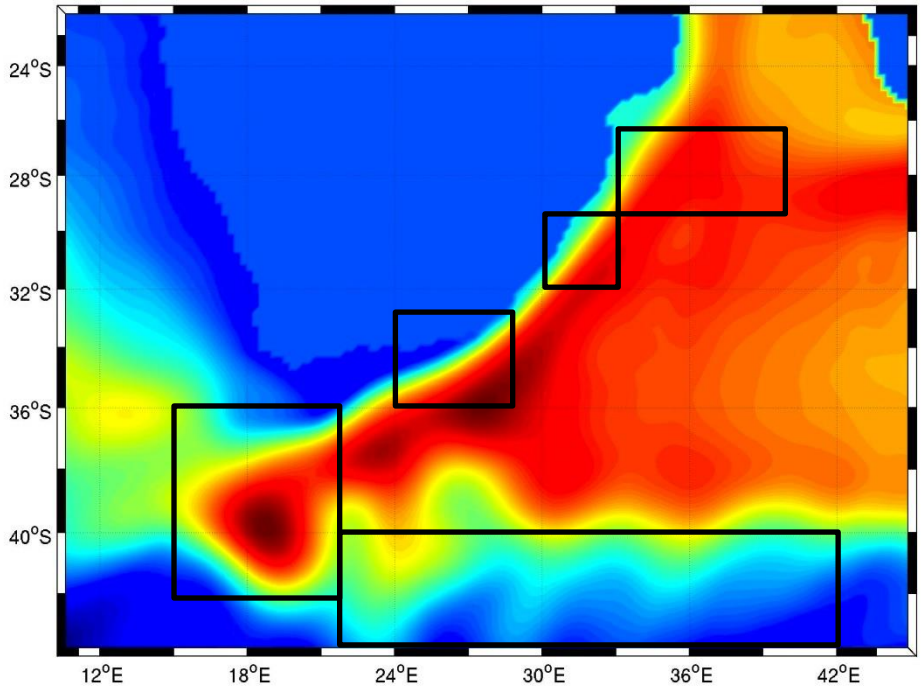

Figure 5.1: Position of the Analysed blocks within the Agulhas region over the mean SSH

The temperature between 150m and 200m depth for the Agulhas region (STF not included) does not show a strong trend over the 60 year time series, except for the South Agulhas and the Agulhas Retroflection region. The South Agulhas shows a negative trend, while the Retroflection shows the most marked increase over the time series (Figure 5.2). All four blocks (Figure 5.2) tend to show negative anomalies in temperature between 1950 and 1956, and positive anomalies between 1960 and 1968. Another period of large positive anomalies occurs between 1990 and 1996, and a period of negative anomalies then follows in 2000 to 2006. The period between 1968 and 1988 appears to contain weak anomalies, suggesting a more stable period in subsurface temperatures, with only the Retroflection

showing an anomalous increase in temperature in the in the early 1980s.

The SSH (Figure 5.3) shows no ostensibly severe trends over the 60 year time series, except in the Retroflection, where there is a positive trend over the time series. There are equivalent decreases between 1950 and 1956 and increases between 1960 and 1968 to the fluctuations seen in the temperature across the blocks. The SSH however increases in the 1990 to 1996 period, decreases slightly, then continues to increase into the 2000 to 2006 period. This behaviour in the 1990s and 2000s anomalous periods is roughly opposite to the fluctuations seen in the temperature over the same time period, however it lacks the ostensible magnitude of the anomalies seen in the 1950s and 1960s periods.

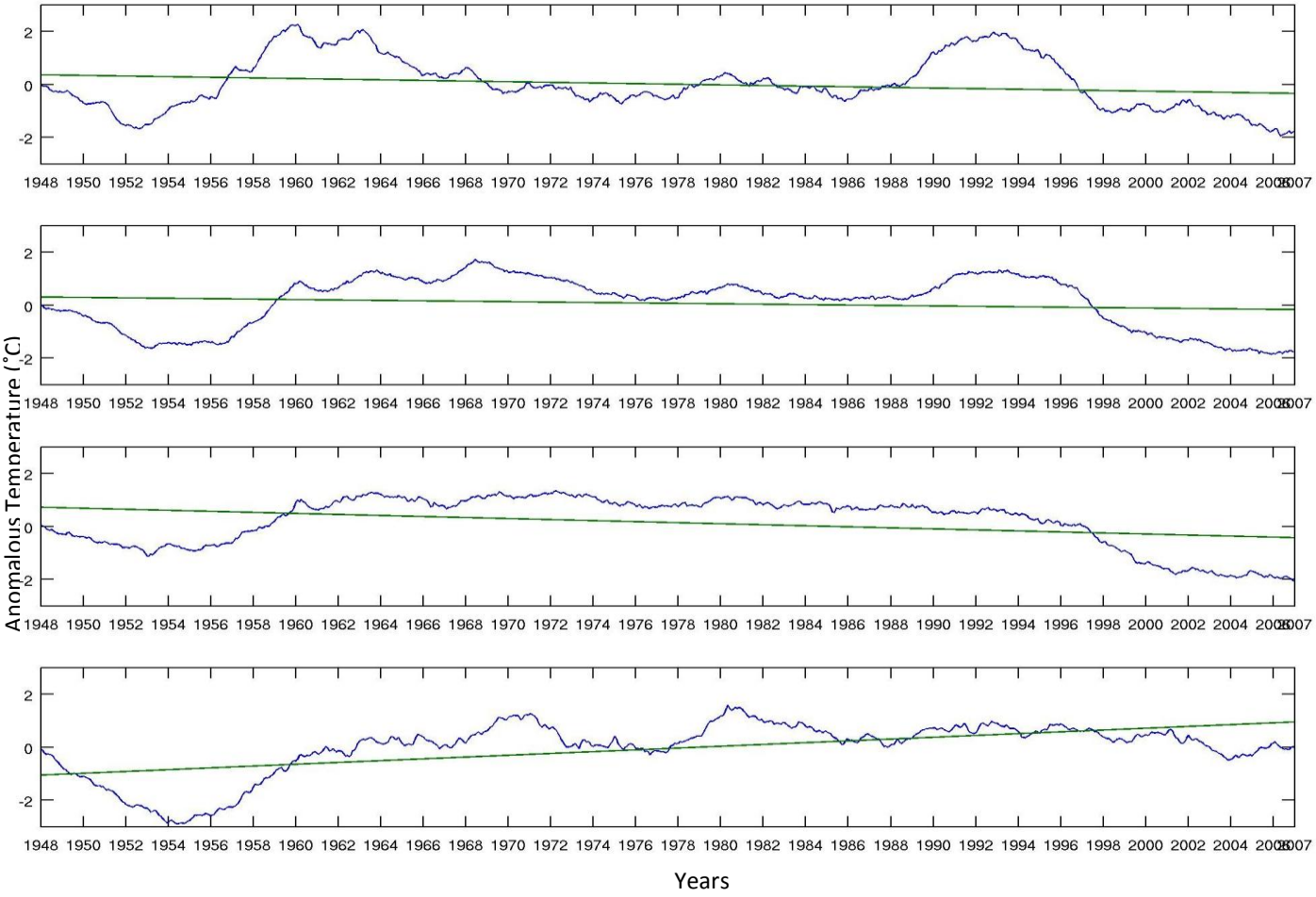

Figure 5.2: Temperature changes for the regions Northern, Central, Southern and Retroflection respectively

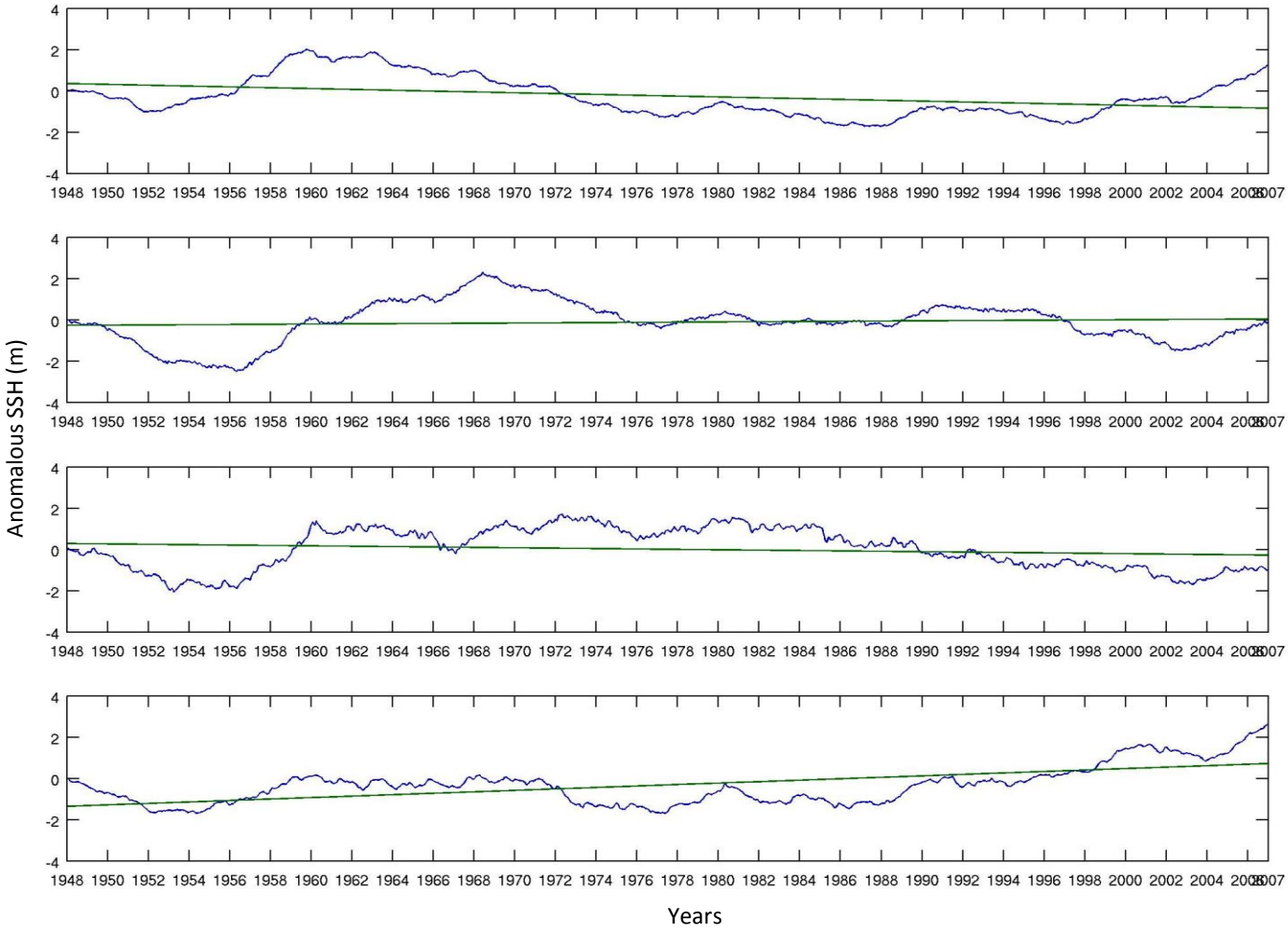

Figure 5.3: Sea Surface Height changes for the region Northern, Central, Southern and Retroflection respectively

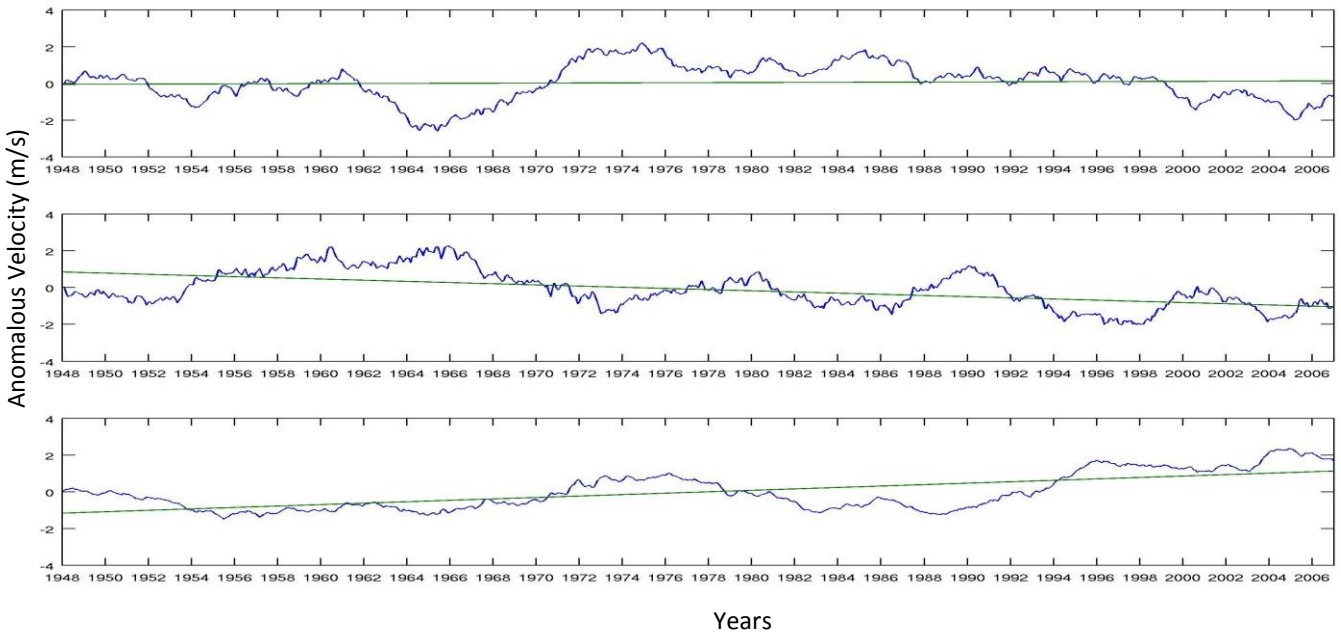

Figure 5.4: Meridional Velocity changes for the regions Northern, Central, and Southern respectively

The meridional velocity anomalies showed little overall trend in the Northern Agulhas block; however there are opposing trends in the Central and Southern Agulhas – a marked overall decrease in the velocity over the 60 year time series in the Central Agulhas, while there is an overall increase in velocity in the Southern Agulhas block. The Central Agulhas block appears to be more variable, with relatively large fluctuations through the time series.

The zonal velocity associated with the STF block (Figure 5.5), tends to increase over the 60 year time series. Figure 5.5 shows the STF velocity to have negative anomalies in the 1950s and positive anomalies in the 1960s, similar to the anomalies in the temperature and SSH in the northerly blocks (Figure 5.2 and 5.3), and the temperature within the STF block (Figure 5.6). The temperature within the STF block shows a similar tendency to the velocity of the STF block – positive anomalies across the time series. The SSH gradient was used to locate the STF position, with the STF being positioned at the area of the averaged highest gradient over the latitiude. Figure 5.7 displays the temperature of the STF block with the STF position superimposed. Visible is the southward shift of the STF with an increasing influx of warmer water flowing in from the north from around 1990.

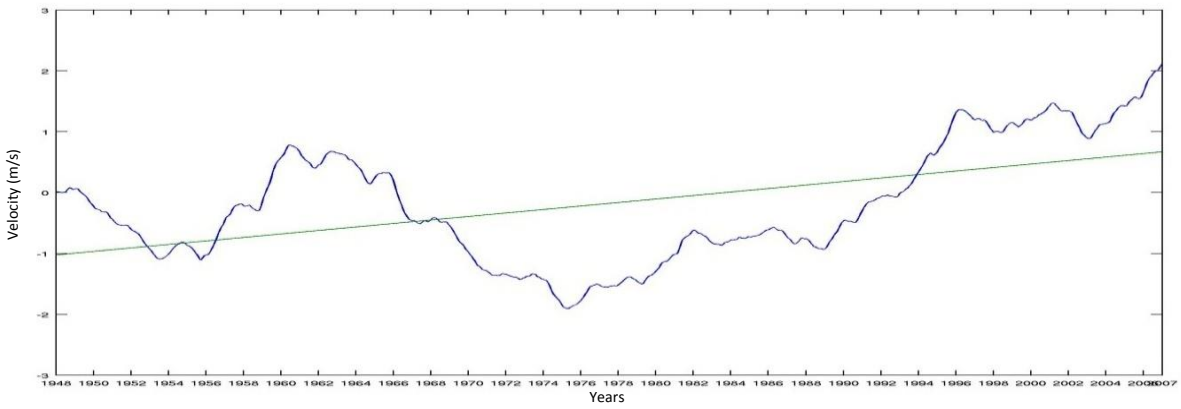

Figure 5.5: Zonal Velocity anomalies for the Agulhas Return Current region over time

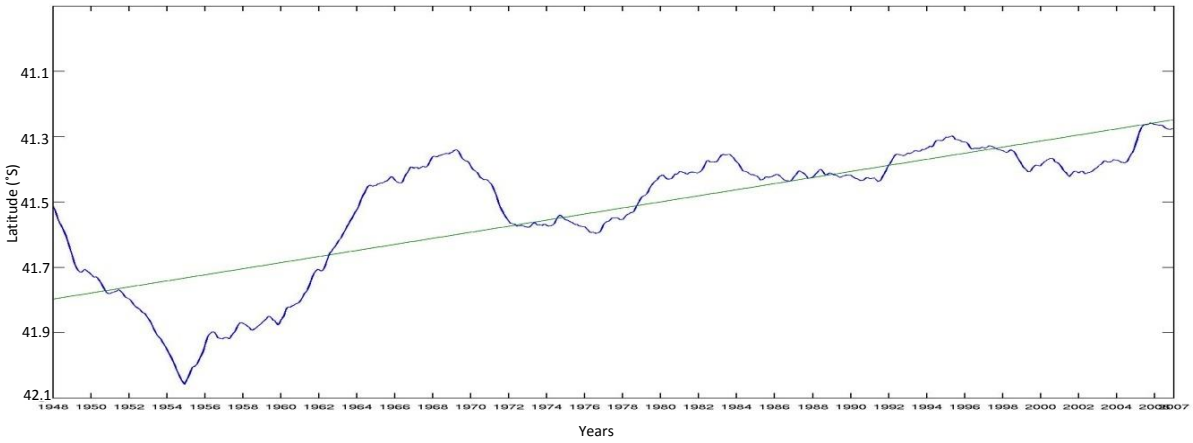

Figure 5.6: Change in the latitudinal position of STF (located using SSH gradient) over time

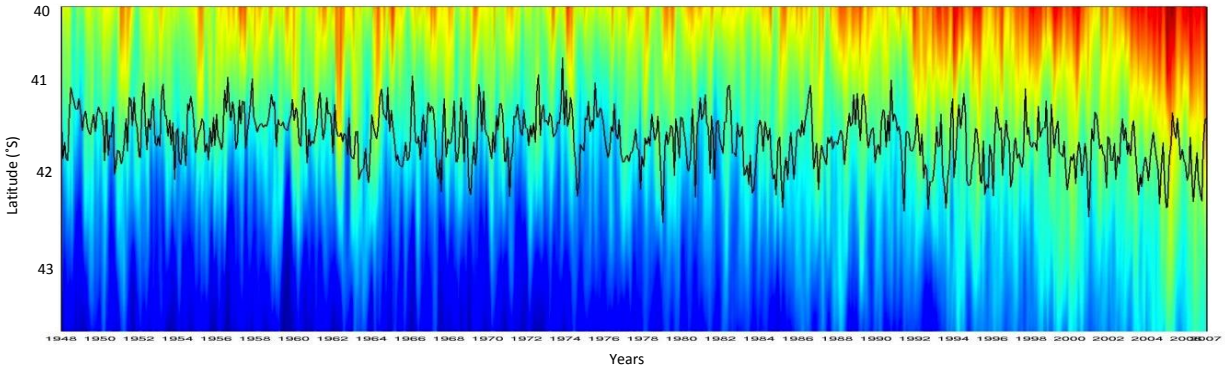

Figure 5.7: Position of the STF with temperature of the region over time

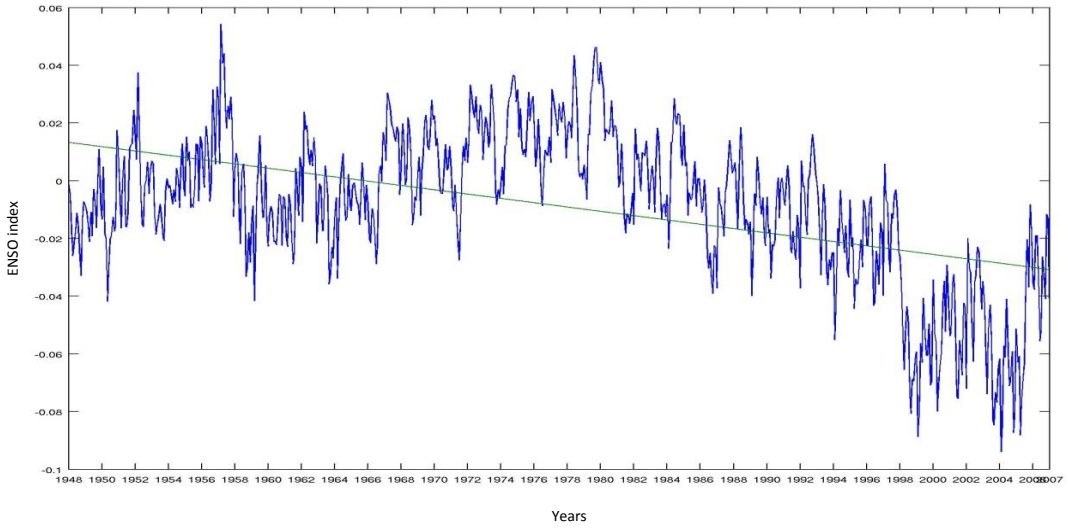

Figure 5.8: Anomalous ENSO Index for 1948 to 2007

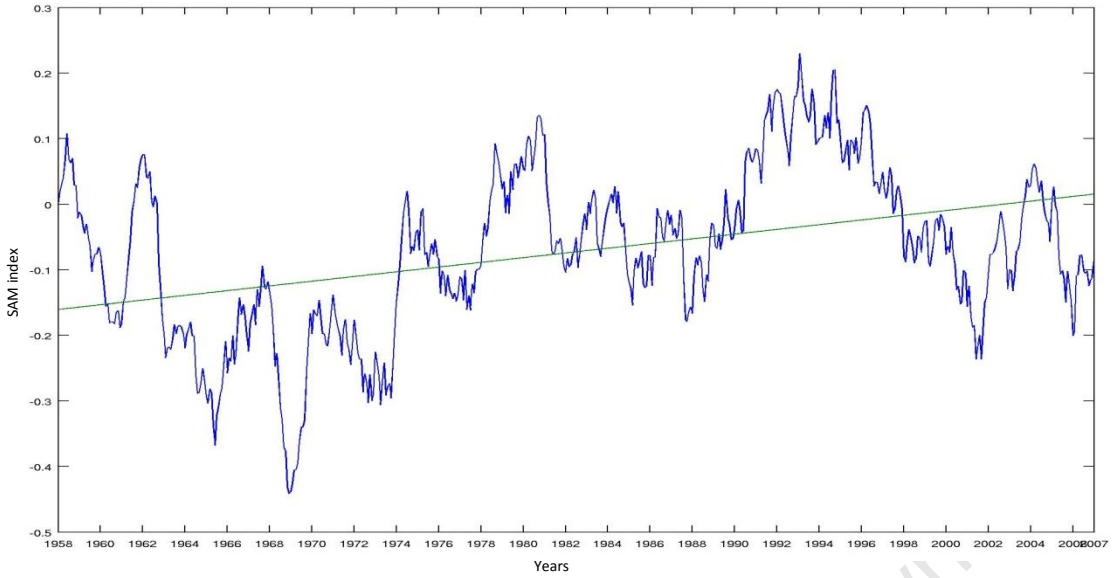

Figure 5.9: Anomalous SAM index 1956 to 2007

Correlations:

The time series of anomalous temperature (at a depth of between 150m and 200m) and SSH anomalies were correlated against indices for ENSO (NINO 3.4) and the SAM (taken from Marshall, 2003) (Figure 5.8 and Figure 5.9). Strong statistical significance (99%) is highlighted in red. These have correlation values of greater than 0.3 or less than -0.3. There is a strong correlation across all lag times for the South Agulhas with ENSO (Table 5.1) - the highest correlation (p-value of 0.000 and R-value of 0.6173) being found at a lag of 6 months. The Central Agulhas also has an increasing strength of correlation with an increasing lag in months (from 0 to 6 months lag). The negative correlation associated with the STF suggests that during El Nino events negative temperature anomalies occur near the STF, and the opposite during La Nina. Colberg *et al.* (2004) find that with a progression of El Nino, there is are induced wind anomalies which alter the heat flux. This may result in a cooling of the SST through mixing. Correlations of temperature with the SAM index are weak: R-values are considered outside of the range of interest (range of interest being 0.3 and above or -0.3 and below).

Table 5.1: R-values of correlations between ENSO and the temperature of the regions with a 0 – 6 month lag on the regions response

	0	1	2	3	4	5	6
North Agulhas	0.1674	0.1714	0.176	0.1796	0.1844	0.1886	0.1941
Central Agulhas	0.3754	0.38	0.384	0.3877	0.3933	0.3966	0.4002
South Agulhas	0.5875	0.5931	0.5988	0.6019	0.6085	0.6131	0.6173
Retroflection	-0.0816	-0.0815	-0.0815	-0.0775	-0.0738	-0.0719	-0.0715
STF	-0.3282	-0.3269	-0.3256	-0.3236	-0.3237	-0.3224	-0.3213

Table 5.2: R-values of correlations between SAM and the temperature of the regions with a 0 – 6 month lag on the regions response

	0	1	2	3	4	5	6
North Agulhas	0.0849	0.0901	0.0913	0.085	0.0881	0.091	0.0909
Central Agulhas	-0.0167	-0.0164	-0.0161	-0.011	-0.0153	-0.0137	-0.0056
South Agulhas	-0.0393	-0.0345	-0.0398	-0.0537	-0.0509	-0.0248	-0.0276
Retroflection	0.0535	0.0527	0.0566	0.0599	0.0419	0.0339	0.0401
STF	0.1401	0.1345	0.1299	0.1242	0.1183	0.1123	0.1047

Table 5.3: R-values of correlations between ENSO and the SSH of the regions with a 0 – 6 month lag on the regions response

	0	1	2	3	4	5	6
North Agulhas	0.0106	0.0038	-0.0037	-0.0079	-0.0157	-0.0212	-0.0259
Central Agulhas	0.2024	0.201	0.1975	0.1975	0.1959	0.1941	0.192
South Agulhas	0.5095	0.5127	0.515	0.5178	0.523	0.527	0.5275
Retroflection	-0.6192	-0.6269	-0.6344	-0.6357	-0.6422	-0.6466	-0.6524

Table 5.4: R-values of correlations between SAM and the SSH of the regions with a 0 – 6 month lag on the regions response

	0	1	2	3	4	5	6
North Agulhas	-0.4507	-0.4479	-0.4425	-0.4359	-0.4316	-0.4273	-0.4224
Central Agulhas	-0.2604	-0.2643	-0.2673	-0.269	-0.2708	-0.273	-0.2747
South Agulhas	-0.2048	-0.2087	-0.213	-0.2185	-0.2222	-0.2234	-0.2256
Retroflection	-0.1124	-0.114	-0.112	-0.109	-0.1094	-0.11	-0.1111

Correlations of SSH with the ENSO (Table 5.3) have greater than 0.5 R-values, and are statistically significant at greater than 99% for the South Agulhas and the Retroflection. However, for the Central and North Agulhas, the correlation coefficients are less than 0.3, and therefore not of relevance. The correlation of SSH with the SAM index returned a conducive negative correlation for the North Agulhas (returning R-values about -0.45 to -0.42) significant at 99%. However the correlations over the other blocks were weak (R-values were not below 0.3.

Periods of relatively large anomalies:

The time periods 1950 to 1956 and 2000 to 2006 show relatively large negative anomalies in temperature over the regions, while the time periods 1960 to 1968 and 1990 to 1996 have large positive anomalies, as seen in Figure 5.2. Similar behaviour is observed for SSH. To further investigate these large anomalies, the differences in sea surface temperature (SST), sea level pressure (SLP), geopotential height (GPH) and zonal winds for the Southern Hemisphere were considered between the 1960-1968 period and 1950-1956, and between the 1990-1996 period and 2000 to 2006 . Difference in the former periods for SST is seen in Figure 5.10. As expected from Figure 5.2, the Agulhas region is warmer during the 1960s period. Elsewhere, the central subtropical and mid-latitude regions of each basin are cooler with positive differences in the other regions. In general, there is a wavenumber 4 pattern in the difference plot together with an annular character. These features are reflected in the SLP difference plot (Fig. 5.11) that shows a positive SAM phase in the 1960s versus the 1950s together with southward shifts and strengthening of the subtropical anticyclones. These patterns are also strongly evident in the 500hPa geopotential height differences (Figure 5.12).

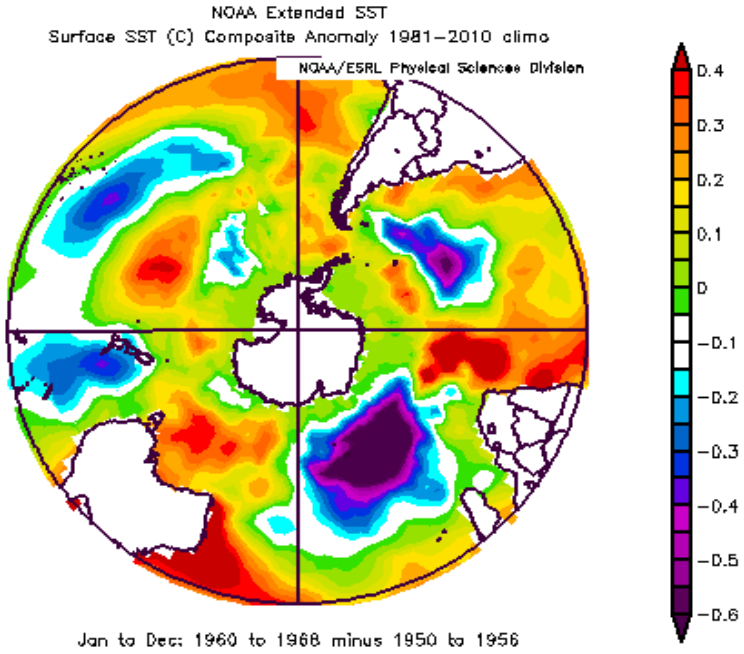

Figure 5.10: The difference in the SST between 1960 to 1968 and 1950 to 1956 (peak period minus trough period)

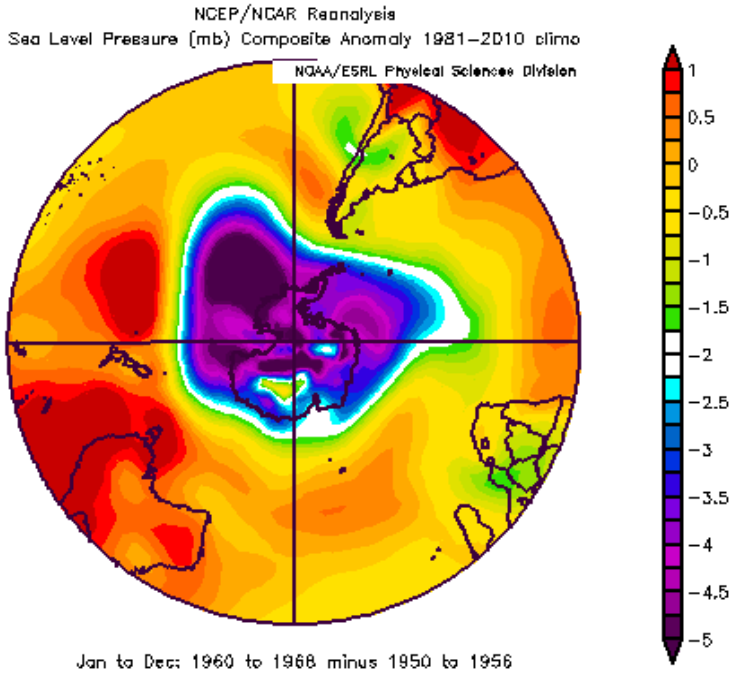

. **Figure 5.11: The difference in the sea level pressure between 1960 to 1968 and 1950 to 1956 (peak period minus trough period)**

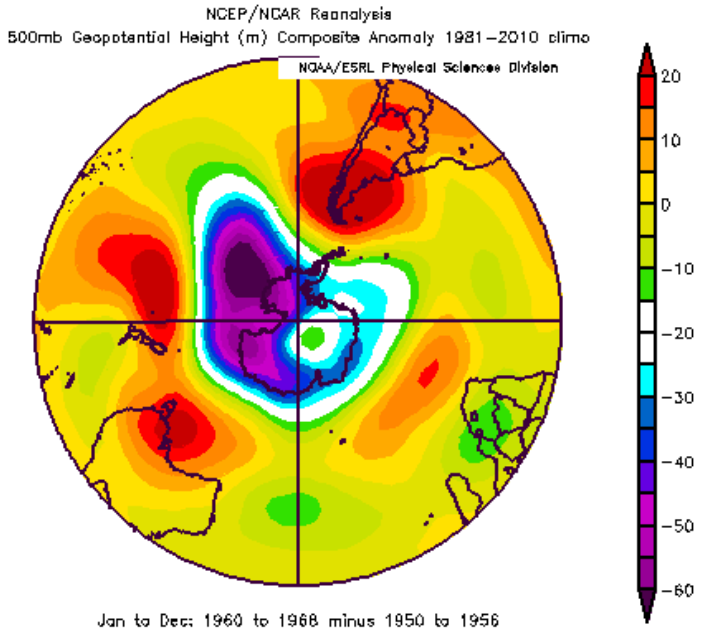

Figure 5.12: The difference in the 500 mb geopotential height between 1960 to 1968 and 1950 to 1956 (peak period minus trough period)

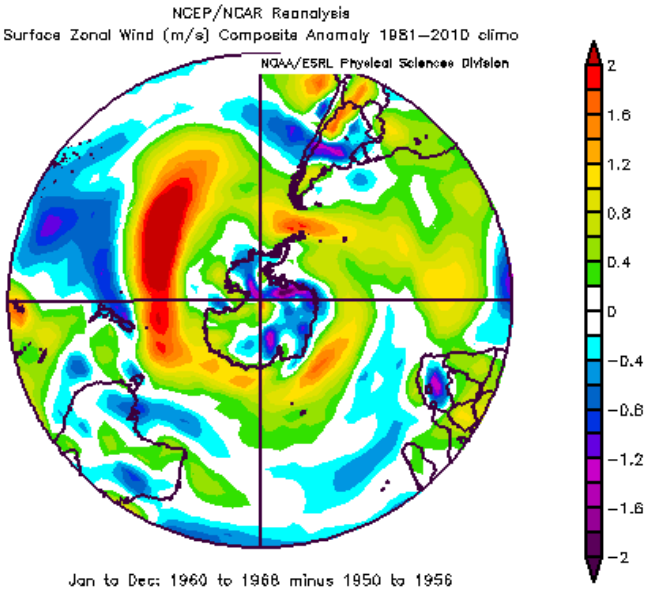

Figure 5.13: The difference in the surface zonal winds between 1960 to 1968 and 1950 to 1956 (peak period minus trough period)

If the anomalies in SSH and upper ocean temperature are mainly as a result of the ocean responding to changes in atmospheric forcing, then changes in surface zonal wind may help explain those in temperature. For example, changes in surface wind may lead to those in Ekman transport, upper ocean divergence / upwelling and in mixing. Figure 5.13 implies stronger westerlies throughout the Southern Hemisphere in roughly the 50-65˚S band during the 1960s are consistent with the positive SAM pattern seen in Figures 5.11-5.12. South of Africa there are weaker westerlies implying less upper ocean mixing and reduced northward Ekman transport and hence warmer upper ocean temperatures. The large region of cooler temperatures in the central South Indian and Atlantic mid-latitudes can be explained to some extent by enhanced Equator-ward Ekman transport from the stronger mid-latitude westerlies.

The SST difference for the 1990s and 2000s period is seen in Figure 5.14. The difference in the sub-surface temperature found in the Agulhas region, is thought to be positive (peak period of the 1990s minus the trough period of the 2000), however Figure 5.14 shows a negative anomaly of SST across the Agulhas region. This anomaly is contrasted with the positive anomalies of SST in the Amundsen-Bellinghausen seas (South Pacific Ocean). This warmer SST is suggested as a result of reduced upper ocean mixing, concurrent with an observed decrease in the surface zonal wind around the 50˚S band (Figure 5.17). This behaviour is contrasted with the cooling of SST across the central and west Pacific. This pattern of SST is suggestive of a positive ENSO or El Nino-like pattern of variability. This is presumed to be due to the occurrence of El Nino and La Nina events: the 1990s contained several El Nino events (Trenberth and Hoar, 1997) and only one weak La Nina, while the 2000s contained a multiple of both El Nino and La Nina events (suggested from the NOAA CPC Nino index, Appendix 1) – this would result in a predominantly El Nino signal from the difference (1990's minus 2000). Negative SST anomalies are located over the Central Indian Ocean, as well as the subtropical Atlantic Ocean. The Central South Indian Ocean, and into the Agulhas region are seen to have negative SST anomalies, presumed to be linked to the increase in wind anomalies found over the same region, as the surface winds may positively influence divergence and mixing, resulting in negative SST anomalies.

While the 1990s and 2000s SLP and GHP differences lack the positive SAM pattern of the 1950s and 1960s period, there is evidence of anomalously positive GPH (Figure 5.16) over the Amundsen-Bellingshausen Seas and south of Africa portraying a weak wavenumber 3 pattern. The SLP (Figure 5.15) shows a positive difference across most of Antarctica, and over the Amundsen-Bellingshausen seas, suggestive of a global forcing, however lacking a distinctive wavenumber. The difference in the SLP for the period shows there to be small regions, in the south-west Pacific, south Indian, and the south Atlantic, that show an increased negative anomalous SLP concurrent with regions of reduced SST. These areas are also marked with an increase in the westerlies, suggestive of upper ocean mixing that would result in a decreased SST.

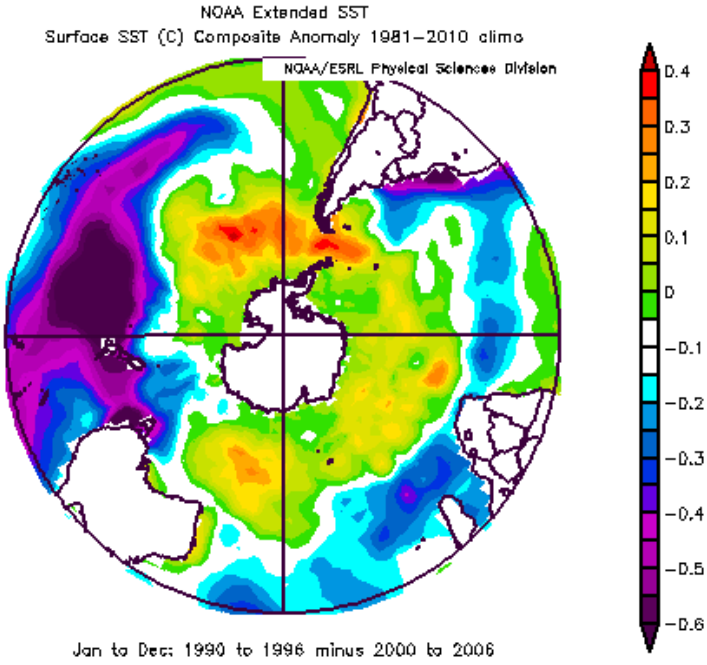

<u>Figure 5.14:</u> Difference in SST between 1990 to 1996 and 2000 to 2006 (peak and trough period)

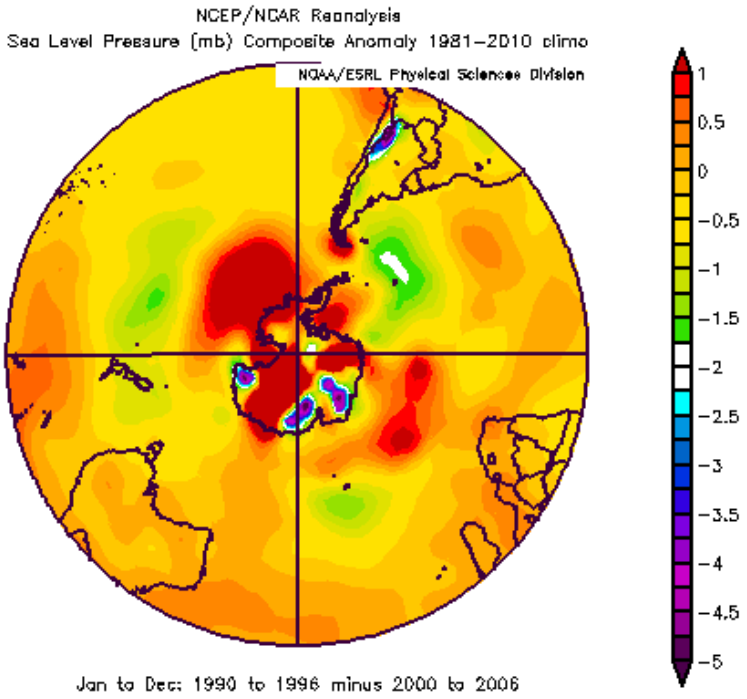

Figure 5.15: The difference in the sea level pressure between 1990 to 1996 and 2000 to 2006 (peak period minus trough period)

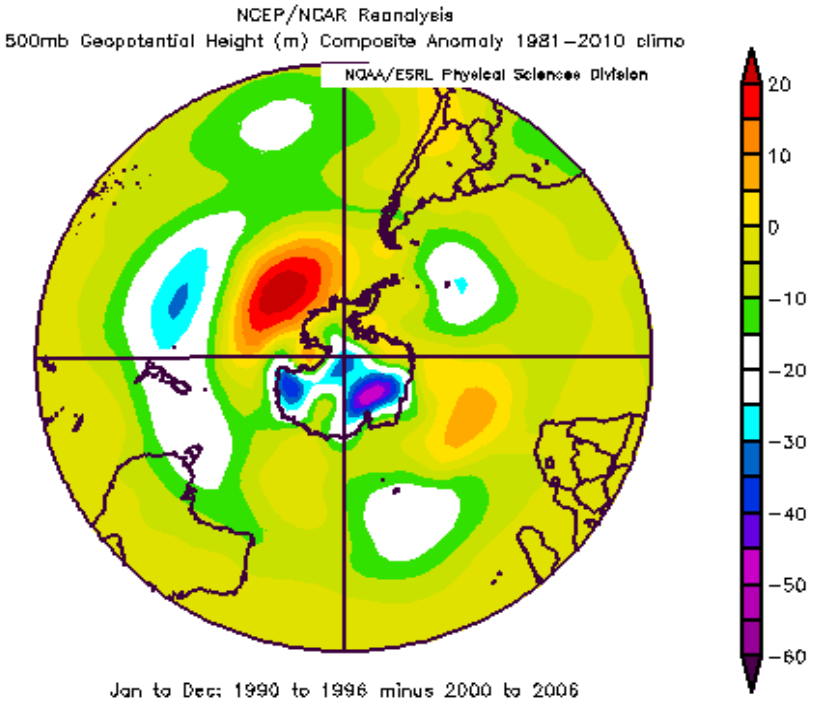

Figure 5.16: Difference in the 500 mb geopotential height between 1990 to 1996 and 2000 to 2006 (peak period minus trough period)

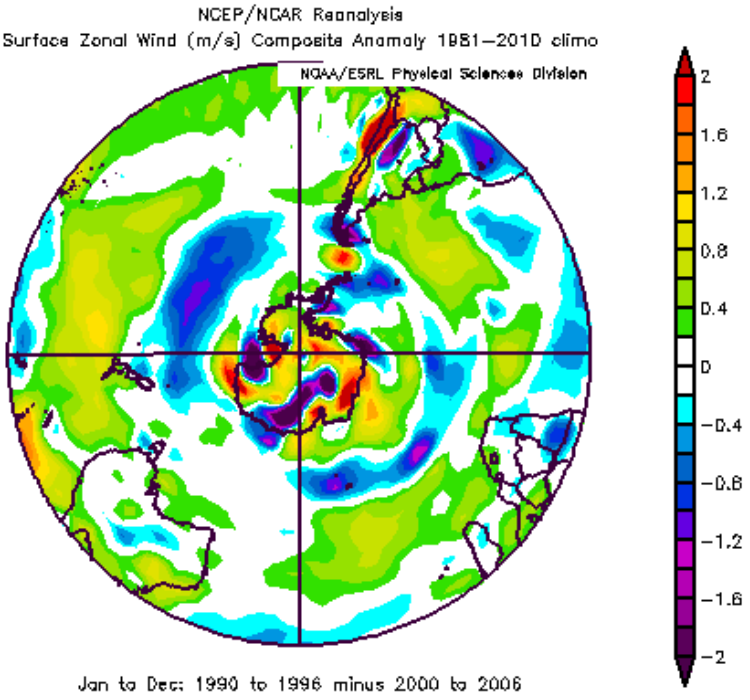

<u>Figure 5.17:</u> The difference in the surface zonal winds between 1990 to 1996 and 2000 to 2006 (peak period minus trough period)

6. Discussion:

The Agulhas current, the western boundary current of the South Indian Ocean, is found by Biastoch *et al.* (2009) and Beal *et al.* (2010) to have global implications in its variability. Beal *et al.* (2011) present evidence that alterations within the current flow of the Agulhas affect the leakage into the South Atlantic, which plays a significant role in the Global Meridional Overturning Circulation (GMOC). The leakage of the Agulhas, in the form of rings into the Atlantic, occurs at the Agulhas Retroflection (Lutjeharms, 2006) and is altered by the flow of the Agulhas current and the position of the Subtropical Front to its south (Beal *et al.*, 2011). Changes in the Agulhas region, indicated in the temperature of the current, sea surface height (SSH) along with velocity of the current, are shown by Backeberg *et al.* (2012) to have an upward trend. The forcing of the variations within the Agulhas is linked to the influence of the modes of variability, the El Niño-Southern Oscillation (ENSO) (Reason *et al.,* 2006) and the Southern Annular Mode (SAM) through its effect on the Subtropical Front (STF) position (Jacobs, 2006; Beal *et al.*, 2011). A distinct understanding of the variability and trends associated with temperature, SSH and velocity and how these link to global forcings is required for an increased understanding of the role this variability within the current plays in the larger GMOC.

Temperature:

Variability in the Agulhas current is found by Backeberg *et al.* (2012) to involve an upward trend. Mesoscale variability across the region is said to have been on the increase from 1993 to 2009 (Backeberg *et al.*, 2012). It is seen in Figure 5.2 that with the modelled data there is not a noticeably strong increase in temperature across the region as none of the blocks contain a strong upward trend. There were periods of increased temperature, such as 1960 to 1968 and 1990 to 1996, and corresponding decreased temperature periods, such as 1950 to 1956 and 2000 to 2006.

The results do not show a strong similarity to the trend found by Rouault *et al.* (2009). Rouault *et al.* (2009) suggest there to be a warming trend in the Agulhas current since the 1980s. While the results show a period of heightened temperature in the 1990s, this is followed by a decrease in temperature in the 2000s hence no warming trend over the entire time series is seen. This is thought to be due to the length of the time series analysed. 60 years is considerably longer than Rouault *et al.* (2009) analysis over 20 years. It is also suggested that the difference between the results and Rouault *et al.* (2009) may be due to the time series results being subsurface (150 m to 200 m) while Rouault *et al.* (2009) analyses sea surface temperature (SST). The SST, being in contact with the atmosphere, is suggested to be more variable and influenced by localized forcings (Molinari *et al*., 1997), while subsurface temperature, out of direct contact with the atmosphere, is a signal of longer term variability (Zhang and Levitus, 1996). Modelled SST is also constrained by the way the model is forced at the surface, thus subsurface temperature was analysed instead. The model validation dictates that the results appear warmer than the actual temperatures found across most of the region, thus corrections are required on the model to replicate exactly temperatures across the region. The implication of the result's minimal trend in long-term variability of temperature in the Agulhas region is such that, with an increase in global climate variability, there appears to be a mediating effect on temperature within the Agulhas region, the cause of this requiring further study. Similarly future studies are suggested to ascertain statistically the significance of trends found within the data.

Sea Surface Height (SSH):

The SSH, similar to that of the subsurface temperature, shows no strong trend over the time series (Figure 5.3). There are peaks and troughs in the data that correspond to those seen in the temperature figure (Figure 5.3). When visually compared to Simple Ocean Data Assimilation (SODA) SSH data (Appendix 11.2) there appears to be a large difference between the two. The SSH results for the same time series (1955 to 2005) (Appendix 11.3) as the SODA SSH show that there are similarities

between the time series when the data is not smoothed. However after smoothing the results using a 7 year running mean, to extract low frequency variability, there is little resemblance to the SODA SSH. This suggests that the low frequency variability signal is hidden amongst higher frequency variability, with a 7 year running mean this high frequency variability is reduced.

Backeberg *et al.* (2012) show evidence that the Agulhas region SSH variability is complex, with a decrease in SSH in the area defined in this project as the Northern Agulhas and Central Agulhas (from 20˚S to 30˚S), while there is an increase downstream of the Agulhas retroflection and in the Agulhas Return current. Visual analysis shows that these trends are seen to some extent in the results - the Northern Agulhas shows a decreasing trend, with an increase in negative anomalies. However the Central Agulhas does not have a negative trend, unlike that found by Backberg *et al.* (2012).This difference from Backeberg *et al.* (2012) may be due to the area of SSH analysed differing from that of Backeberg *et al.* (2012), as well as different data processing between these results and the results by Backeberg *et al.* (2012). There is a decreasing trend in the Southern Agulhas (33˚S to 36˚S), which is in agreement with the tentative findings of Backeberg *et al.* (2012), the wave pattern being less visible, but indicating a decrease in the trend across the latitudes 30˚S to 40˚S. The Retroflection block is found to have an increasing trend, due to the increasing positive anomalies, consistent with Backeberg *et al.* (2012). The changes in the SSH are attributed by Billany *et al.* (2010) to changes in the wind stress curl, the driver of ocean circulation. The changes in SSH as a proxy for changes in transport (Backeberg *et al.*, 2012) suggest an alteration of the forcings on the Agulhas region, along with an alteration in flow. A change in the Retroflection is found by Beal *et al.* (2011) to have global implications in circulation, thus with an increase in SSH within the Retroflection, there is a required a further study of the global effect of a change in the leakage of the Agulhas, along with quantifying the extent of the variation.

Velocity:

The meridional velocity in the Agulhas shows contrasting trends in the anomalies, with the Central Agulhas showing a decrease in the velocity anomalies (negative trend) as seen in Figure 5.4. The decrease in anomalies may be explained by the findings of Backeberg *et al.* (2012), who suggest that the area may be moving towards an increased mean energy and a reduction in eddy energy. This is contrasted with the meridional velocity anomalies in the Southern Agulhas which show an increase in the meridional velocity anomalies. Backeberg *et al.* (2012) relates this to increased turbulence and contribution to the Agulhas current's energy by eddies. These changes in velocity, similar to those seen in SSH, are connected to alterations in wind stress curl which in turn is linked to large scale circulation such as El Niño-Southern Oscillation (ENSO) and Southern Annular Mode (SAM) (Reason *et al.,* 2000; Cai *et al.*, 2005). The Agulhas Return current and the Subtropical Front (STF) show an increase in positive zonal velocity anomalies (Figure 5.5) along with a northward shift in the STF position (Figure 5.6). This increase in trend in the velocity would suggest an increase in the wind stress curl over the South Atlantic – Southern Ocean (the region responsible for a part of the forcing behind the Antarctic Circumpolar Current, and thus the flow along the STF and Agulhas Return current) (Orsi *et al., 1995*). The increase in wind forcing responsible for the increased positive velocity anomalies is suggested to be the cause of the northward shift of the STF, with Billany *et al.* (2010) noting that increased wind stress curl over the South Atlantic results in a northward shift of the southern ocean frontal positions, as seen in Figure 5.6 with the northward movement of the STF. A variation in the STF's position will alter the Agulhas leakage (Beal *et al.*, 2011). A northward shift in the STF is found to narrow the Retroflection region and reduce leakage of Agulhas water into the Atlantic (Beal *et al.*, 2011). Thus the northward trend seen in Figure 5.6 has global implications in ocean circulation, however there has yet to be a quantifiable understanding of these implications. With the northward shift of the STF there is seen a southward creep in warmer subsurface temperature, as seen in Figure 5.7, however the south of the block remains as cool as in the beginning of the time

series. This localized warming in the north of the block later in the time series (1992 to 2007) is suggested to increase the temperature gradient across the block, and thus the SSH gradient, adding to the increase of the positive velocity anomalies and attributing to the northward shift of the STF's position. Beal *et al.* (2011) states that with a northward shift in the STF there is expected to be a decrease in the leakage, however this is only if the flow remains constant. It is suggested that for future studies, an integration of the meridional and zonal velocity is required as a large portion of the Agulhas current flows in the south-west direction. Therefore an integrated velocity would provide a clearer understanding of the Agulhas Current.

Correlations:

Correlations performed on the unsmoothed data did not return any significant correlations with either the El Niño – Southern Oscillation (ENSO) anomalies index (NINO 3.4 data) or the Southern Annular Mode (SAM) anomalies index. This is thought to be due to the highly variable nature of the Agulhas region (Lutjeharms *et al.,* 2012). The 7-year running mean applied to the subsurface temperature and the SSH anomalies then correlated with ENSO and SAM anomalies from a 0 to 6 month lag time. Significant correlations (with a p-value of 0.05 or less) were considered relevant if the R-value was higher than 0.3 (positive correlation) or lower than -0.3 (negative correlation). Correlations were not performed for SSH over the STF region as SSH was used to locate the position of the STF.

The Northern Agulhas, although having significant p-values (0.000), does not return high R-values. The Central and Southern Agulhas subsurface temperature anomalies, however, show strong correlations with ENSO anomalies, with the strongest correlation occurring in the Southern Agulhas at the 6 months lag (p-value of 0.000 and R-value of 0.6173). This increase in positive correlation with an increase of 6 months of lag time is in accordance with Reason *et al.* (2000) who show evidence for a one season lag before El Niño/ La Niña modes are displayed in the South Indian Ocean, and hence the Agulhas region. The STF block is found to have a negative

correlation with ENSO anomalies (Table 5.1). With an increase in the ENSO anomalies, there is a decrease in the temperatures associated with the Agulhas Return current and the STF. This unusual negative anomaly is suggested as being a result of the influence of the Southern Ocean on the block's subsurface temperatures as Colberg *et al.* (2004) show evidence that with an El Niño (La Niña) mode, there are negative (positive) temperature anomalies associated with the South Atlantic and the Southern Ocean. Thus while correlations near the source region of the Agulhas (the Northern Agulhas) and ENSO do not return strong correlations (above 0.3), the Central and Southern Agulhas and the STF blocks show there to be correlations with ENSO anomalies, and thus display a connection between the large scale variability of the atmosphere and the variability associated with the Agulhas region.

The correlation of anomalous subsurface temperature with the anomalous SAM index shows only significant p-values (0.05 or less) in the Northern Agulhas and the STF blocks, however the correlations were not strong enough to return R-values greater than 0.3 or less than -0.3. Thus while there is a correlation between SAM and subsurface temperature across the Agulhas region, the correlation is not a strong one. This is considered unusual, as the SAM is thought to have a stronger influence with increasing latitude (Marshall, 2003). A possible cause of this weakening correlation with increasing latitude may be attributed to the time series of SSH – the Southern Agulhas block, and the Retroflection both contain high fluctuations, even within the 7 year running mean. These fluctuations may skew the results to a weak correlation.

The SSH for the blocks within the Agulhas, correlated against ENSO, show there to be a significant, strong correlation with the South Agulhas and the Retroflection (p-values of 0.000 and R-values greater than 0.3 for the South Agulhas, and less than -0.03 for the Retroflection). The South Agulhas shows a positive correlation with the ENSO, similar to the correlation seen in the subsurface temperature. This correlation

is attributed to the changes in wind stress curl caused by changes in the ENSO index. Rasmusson and Carpenter (1982) note that ENSO is associated with a change in wind stress curl globally and thus with an alteration in the wind stress curl, which is a determining factor in the driving of currents and SSH (Backeberg *et al.*, 2012), there can be expected a strong correlation between the SSH and ENSO. However the lack of a strong correlation in the Central Agulhas block, and the lack of significance in the Northern Agulhas, is unusual. This may be attributed to the turbulence associated with the source of the Agulhas thus there is no clear signal from the impact of ENSO, however there is no proof of this. The weak SSH-ENSO correlation seen in the Central Agulhas (p-values of 0.000, but R-values less and 0.3) is similar to that seen in the temperature-ENSO correlation for the same region. The cause of this weak SSH correlation with ENSO in the Central Agulhas, across all lag times, is thought to be a result of the Central Agulhas being placed between the Northern Agulhas block, with no correlation to ENSO, and the Southern Agulhas block, with a strong ENSO correlation. The Retroflection block, to the west of the Southern Agulhas, showed a negative correlation of SSH anomalies with ENSO anomalies (p-values of 0.000) over all lag months. The correlations strengthen across the increased lag months starting with an R-value of -0.6192 at 0 months lag, and ending with a R-value of -0.6524 at a 6 month lag time. A negative correlation with ENSO was seen in the subsurface temperature, however it lacked the strength of the SSH correlation. The exact reason for the negative correlation between SSH and ENSO is unknown, however it is noted by Beal *et al.* (2011) that an alteration in wind fields, suggested as associated with ENSO, results in a shift of the Agulhas Retroflection. Therefore with a positive ENSO anomaly, and the associated changes in the wind pattern this may cause the Agulhas Retroflection to shift outside the Retroflection block (the block used for the correlation) and thus causing negative anomalies in SSH within the analysed Retroflection block.

Correlations of SSH with anomalous SAM indices returned statistically significant results across all of the blocks, however only the Northern Agulhas contained what is

considered strong correlations (R-values higher than 0.3). The Northern Agulhas, having not correlated strongly with the SAM in the temperature-SAM correlation, shows a correlation between SSH and SAM, with the strongest correlation occurring at the 0 months lag time. This positive correlation is unusual in that while Marshall (2003) suggests that there might be a positive trend found in the SAM index, however the Northern Agulhas SSH is found, in this study and by Backeberg *et al*. (2012), to contain a slight negative trend in the SSH anomalies. The correlation with SSH and SAM across the region is expected - the SAM influences sea level pressure (SLP) (Rogers and van Loon, 1982) and hence SSH across the southern hemisphere. With an increased SAM index, there is a decrease in SLP and a resulting increase in SSH. Thus it is expected that there is a positive correlation between SAM and the SSH within the Agulhas region. The strongest correlation occurring at a lag time of 0 months is an indication that the influence of SAM on the northern Agulhas is direct, suggested as being the SLP altering the SSH, however the weak correlations found in the blocks south of that are again unusual, and suggestive as being attributed to the fluctuations found in the SSH time series.

The implication is that with significant correlations linking parts of the Agulhas region to the global circulation modes ENSO and the SAM, and increased anomalies within these modes in recent years (Trenberth and Hoar, 1997), it is expected that there will be resulting variations in the Agulhas region that will in turn affect rainfall over Southern Africa (Reason *et al.*, 2006) along with altering the influence the Agulhas region has on global ocean circulation (Beal *et al.*, 2011). However the connection between ENSO/the SAM and the Agulhas region requires a greater depth of understanding, as the mechanisms, resulting in sections of the Agulhas region having strong correlations while other sections do not, are poorly understood.

Periods of Relatively Large Anomalies:

The time series of both sub-surface temperature (Figure 5.2) and the SSH (Figure 5.3) show there to be periods of heightened anomalies within the 60 years. There is an

increase in positive anomalies seen in 1960 to 1968 and 1990 to 1996, while the periods 1950 to 1956 and 2000 to 2006 show increased negative anomalies. The difference between the periods 1960-1968 (peak in anomalies) and 1950-1956 (trough in anomalies) for sea surface temperature (SST), sea level pressure (SLP), 500 mb geopotential height (GPH) and zonal surface winds seen in Figures 5.8 to 5.11 show a potential cause of the heightened anomalies between the two periods.

SST in the Central Indian Ocean appears to be higher in the trough period (1950 to 1956) than in the peak period (1960 to 1968), while the SLP and GPH differences between the peak and trough period show similar atmospheric wave patterns. The GPH shows clearly a wavenumber 4 pattern, while the SLP shows a wavenumber 3 or 4. This wavenumber, as a symmetrical pattern with a strong gradient between the region over Antarctica and the subtropics, is suggested by Carlton (2003) to be the result of the SAM forcing on the global SLP and GPH. SAM is more evident in the region of the 500mb GPH (Rogers and van Loon, 1982) highlighting that the variation in anomalies between the peak and the trough period may be associated with the SAM index. The surface zonal wind difference (Figure 5.11) between the peak and trough periods again suggests a connection to the SAM, with strong positive wind anomalies across the regions of increased SLP and GPH gradient that point to a SAM-forced wavenumber 4. The change in the Agulhas region is thought to be an interplay of the SLP and the zonal wind: alteration in the SLP will lead to a fluctuation in the SSH within the Agulhas region, while it is found by Ekman (1905) and Price *et al.* (1987) that zonal winds play a role in variability of both transport and temperature. Thus it is assumed that the fluctuation between the trough and peak periods is as a result of the SAM forcing, visible in the SLP, GPH and zonal winds.

The other peak and trough periods are 1990 to 1996 and 2000 to 2006 respectively. Between the peak periods (1990 to 1996) and the trough periods (2000 to 2006) SSTs the difference is noticeably warmer SSTs found in the Amundsen-Bellingshausen Seas (located in the South Pacific). The same region also appears to

have an area of increased pressure, seen in the SLP difference (Figure 5.13). This increased temperature and SLP is suggested to be related to shifting ENSO anomalies, as changes in height of Rossby waves (or atmospheric pressure waves) over the Amundsen-Ross Seas has been found by Turner (2004) to be related to ENSO. With the region of high SLP located over the Amundsen-Bellingshausen Seas, there is a region of high SLP found south of Africa. The GPH difference (Figure 5.14) is similar to that of the SLP difference however there is little evidence of the same strength of wave pattern as seen in the previous peak-trough comparison. The 1990 to 1996 and 2000 to 2006 differences also appears more muted than the 1960 to 1968 and 1950 to 1956 differences, with the majority of the Southern Hemisphere SLP appearing to have a weak difference between the anomalous periods.

The increase in SLP and GPH over the Amundsen-Bellingshausen Seas and the region south of Africa indicate there may be a wavenumber 2 or 3 pattern of atmospheric variability. Carlton (2003) notes that a wavenumber 2 is largely the result of ENSO forcings, however an El Niño event is associated with a low SLP over the Amundsen Sea – opposite to that found in the peak-trough difference. It is suggested that the pattern seen in the peak-trough difference may be a result of an interplay between ENSO and the SAM. The surface zonal wind difference for this peak-trough period shows a band of positive velocities across the subtropics (Figure 5.15), suggested as the cause of the SST pattern seen. Reason *et al*. (2000) show that SST changes evolve as responses to changes in cloud cover and wind strength. The negative SST anomalies found in the western South Indian Ocean and over the Agulhas region confirm this as there are positive wind anomalies for the same region, suggesting a strengthening of the gyre, increasing mixing, and a cooling of SST over the area, similar to that found by Reason *et al.* (2000) to be forced by ENSO. The difference in the negative SST anomalies over the Agulhas (Figure 5.12) and the positive subsurface temperature anomalies calculated in the results (Figure 5.2) is attributed to the subsurface temperatures having a slower response time, receiving signals of ENSO through Ekman pumping (Reason *et al.*, 2000).

While the SLP for the 1990s/2000s period does not show a distinct high pressure over Antarctica and low pressure over the lower latitude that would indicate a positive SAM, there is evidence of increased pressure associated with the Antarctic (Figure 5.13). The GPH, with a drop in height over Antarctica along with an expected drop seen in the regions of decreasing SLP, is suggested as displaying a weak wavenumber 2 or 3. The positive anomalies in GPH and SLP over the regions of positive SST are mimicked by the negative anomalies in westerly winds over those same areas, as expected. The SLP pattern shows a negative anomaly in the South West Atlantic, which Colberg *et al*. (2000) associate with a strengthening of the mid-latitude westerlies as a continuation of an El Niño forcing. There is a positive anomaly of westerly winds found in that region, in agreement with Colberg *et al.* (2004). The pattern of GPH and SLP indicate that while the SAM and ENSO are seen to influence the Agulhas current, due to the interplay of non-synchronous wavenumber patterns, the resultant variability is muted if there are contrasting influences. Reason *et al.* (2000) argue that any superposition of anomalous SST patterns in the low frequency and the quasi-biennial bands of variability results in an annulment of the Indian Ocean east-west dipole. This overlap of signals within differing bands is suggested as having occurred in this period of anomalies, resulting in a diluted ENSO signal over the Southern Hemisphere.

It appears that while some peak/trough differences in the temperature and SSH time series for the Agulhas region can be attributed to forcings relatively simply, through analysis of the determining factors of the forcing such as SLP and GPH. However, there remains forcings that are not entirely understood, such as that seen in the 1990s/2000s difference. Thus recommended is a test for a level of significance to the difference in peak/trough values, to determine the relevance of the difference from the general variability.

7. Conclusion:

Thus analysis of the Agulhas Current region, through temperature, sea surface height (SSH) and velocity shows periods of heightened positive and negative anomalies, however the trend over the entire time period (1948 to 2007) does not mimic previous research, returning no strong trend across all blocks (Northern Agulhas, Central Agulhas, Southern Agulhas and Retroflection blocks) within the Agulhas region. The study suggests that over the 60 year time series there is no positive or negative trend in temperature, SSH and velocity anomalies.

Analysis did return a strong correlation of the smoothed time series of temperature and SSH with El Niño – Southern Oscillation (ENSO) and the Southern Annular Mode (SAM) within certain blocks. This correlation with particular blocks, as well as with lag times of up to six months is suggested to be a result of the high variability associated with the Agulhas region. This high variability with the correlations across the blocks over different lag times calls for further research into the forcings behind the correlations.

While the time series does not contain a uniform trend across all blocks within the region, there were decades of both heightened negative and positive anomalies found within the time series. These decades are linked to ENSO modes along with the SAM, found through analysis of sea level pressure (SLP), geopotential height (GPH) and surface zonal winds. These modes suggest at a complex link between the blocks within the Agulhas and the modes, as while the defining patterns of the modes associated with the periods, there is potential for further research into the connections between the Agulhas region and the influence over selective periods of ENSO and the SAM. Future studies are required for a firmer understanding of the effect ENSO and the SAM trends have on the region. While the model differs from the WOA data, this difference is constant, and the model is able to return a time series useful in the understanding of the forcings and mechanisms relating to the region.

8. Acknowledgements:

First and foremost, considerable thanks go to Chris Reason, supervisor over the project, along with Ben Loveday for providing the model data and assisting in the data analysis. Further thanks are due to Sue du Plessis, Stephen Doucette-Riise and Eleanor Peplow for assisting in the polishing of the project. Finally, the project would not have been possible without the financial support of ACCESS and the University of Cape Town.

9. Reference List:

ALEXANDER, M.A., BLADE, I., NEWMAN, M., LANZANTE, J.R., LAU, N.C., SCOTT, J.D. 2002. The atmospheric bridge: The influence of ENSO teleconnections on air-sea interactions over the global oceans. *Journal of Climate* 15(16): 2205 – 2231

BACKEBERG, B.C., PENVEN, P., ROUAULT, M. 2012. Impact of intensified Indian Ocean winds on mesoscale variability in the Agulhas system. *Nature Climate Change* 2: 608 – 612

BEAL, L.M., DE RUIJTER, W.P.M., BIASTOCH, A., ZAHN, R. 2011. On the role of the Agulhas system in ocean circulation and climate. *Nature* 472: 429 – 436

BEAL, L.M., CHERESKIN, T.K., LENN, Y.D., ELIPOT, S. 2006. The Sources and Mixing Characteristics of the Agulhas Current**.** *Journal of Physical Oceanography* 36: 2060 – 2074

BELKIN, I.M. and GORDON, A.L. 1996. Southern Ocean Fronts from the Greenwich meridian to Tasmania. *Journal of Geophysical Research* 101(C2):3675-3696

BIASTOCH, A., BÖNING, C.W., SCHWARZKOPF, F.U., LUTJEHARMS, J.R.E. 2009. Increase in the Agulhas Leakage due to poleward shift of the Southern Hemisphere westerlies. *Nature* 462: 495 – 498

BILLANY, W., SWART, S., HERMES, J., REASON, C.J.C. 2010. Variability of the Southern Ocean fronts at the Greenwich Meridian. *Journal of Marine Systems* 82: 304 – 310

BOUDRA, D.B. and DE RUITJER, W.P.M. 1986. The wind-driven circulation of the South Atlantic-Indian Ocean II. Experiments using a multi-layer numerical model. *Deep Sea Research Part A. Oceanographic Research Papers* 33(4): 447 – 482

BRYDEN, H.L., BEAL, L.M., DUNCAN, L.M. 2005. Structure and Transport of the Agulhas Current and its Temporal Variability**.** *Journal of Oceanography* 61: 479 – 492

BURLS, N.J. and REASON, C.J.C. 2006. Sea surface temperature fronts in the midlatitude South Atlantic revealed by using microwave satellite data. *Journal of Geophysical Research* 111: 1 – 13

CAI, W., SHI, G., COWAN, T., BI, D., RIBBE, J. 2005. The response of the southern annular mode, the East Australian Current, and the southern mid-latitude ocean circulation to global warming. *Geophysical Research Letters* 32(23)

CARLTON, A.M. 2003. Atmospheric teleconnections involving the Southern Ocean. *Journal Geophysical Research* 108(C4): 7.1 - 7.15

COLBERG, F., REASON, C.J.C., RODGERS, K. 2004. South Atlantic response to El Niño-Southern Oscillation induced climate variability in an ocean general circulation model. *Journal of Geophysical Research* 109(C12):C12015

DE RUIJTER, W. 1982. Asymptotic analysis of the Agulhas and Brazil Current systems. *Journal of Physical Oceanography* 12(4)

DE RUIJTER, W.P.M, RIDDERINKHOF, H., SCHOUTEN, M.W. 2004. Variability of the southwest Indian Ocean. *Philosophical Transactions of the Royal Society* 363: 63 – 76

DE RUIJTER, W.P.M., VAN LEEUWEN, P.J., LUTJEHARMS, J.R.E. 1999. Generation and Evolution of Natal Pulses: Solitary Meanders in the Agulhas Current. *Journal of Physical Oceanography* 29: 3043 – 3055

DURGADOO, J.V., LOVEDAY, B.R., REASON, C.J.C., PENVEN, P., BIASTOCH, A. 2013. Agulhas leakage response preferentially to a westerlies increase. *Journal of Physical*

Oceanography (In Preparation)

EKMAN, W.V. 1905. On the influence of the earth's rotation on the ocean currents. *Ark. Mat. Astron. Fys* 2: 1 – 53

GILLETT, N.P., KELL, T.D., JONES, P.D. 2006. Regional climate impacts of the Southern Annular Mode. *Geophysical Research Letters* 33

GORDON, A.L., WEISS, R.F., SMETHIE, W.M.Jr., WARNER, M.J. 1992. Thermocline and Intermediate Water Communication between the South Atlantic and Indian Oceans. *Journal of Geophysical Research* 97(C5): 7223 – 7240

GRUNDLINGH, M.L. 1980. On the volume transport of the Agulhas Current. *Deep Sea Research* 27: 557 – 563

GRUNDLIGH, M.L. 1988. Review of cyclonic eddies of the Moçambique Ridge Current. *South African Journal of Marine Science* 6(1): 193 – 206

HAIDVOGEL, D.B. and BECKMANN, A. 1999. Numerical ocean circulation modelling. *London: Imperial College Press*

HALL, A. and VISBECK, M. 2002. Synchronous Variability in the Southern Hemisphere Atmosphere, Sea Ice, and Ocean Resulting from the Annular Mode. *Journal of Climate* 15: 3043 – 3057

HARRISON, D.E. and LARKIN, K. 1998. El Nino-Southern Oscillation sea surface temperature and wind anomalies, 1946-1993. *Reviews of Geophysics* 36(3): 353 – 399

HARTMANN D.L. and LO, F. 1998. Wave-Driven Zonal Flow Vacillation in the Southern Hemisphere. *Journal of Atmospheric Sciences* 55: 1303 – 1315

JACOBS, S. 2006. Observations of change in the Southern Ocean**.** *Philosophical Transactions of The Royal Society* 364: 1657 – 1681

JACOBS, S.S. and GEORGI, D.T. 1977. Observations on the southwest Indian/Antarctic Ocean. *Deep Sea Research* 24: 43 – 84

JAMES, C., TOMZCAK, M., HELMOND, I., PENDER, L. 2002. Summer and winter surveys of the Subtropical Front of the southeastern Indian Ocean 1997 – 1998. *Journal of Marine Systems* 37: 129 – 149

KALNAY, E., KANAMITSU, M., KISTLER, R., COLLINS, W., DEAVEN, D., GANDIN, L., IREDELL, M., SAHA, S., WHITE, G., WOOLLEN, J., ZHU, Y.,LEETMAA, A., REYNOLDS, R., CHELLIAH, M., EBISUZAKI, W., HIGGINS, W., JANOWIAK, J., MO, K.C., ROPELEWSKI, C., WANG, J., JENNE, R., JOSEPH, D. 1996. The NCEP/NCAR 40-year reanalysis project. *Bulletin of the American meteorological Society*, *77*(3): 437- 471

KAPLAN, A., CANE, M., KUSHNIR, Y., CLEMENT, A., BLUMENTHAL, M., RAJAGOPALAN, B. 1998. Analyses of global sea surface temperature 1856-1991. *Journal of Geophysical Research* 103(18): 567 – 589

LARGE, W.G. and YEAGER, S.G. 2004. Diurnal to decadal global forcing for ocean and sea-ice models: the data sets and flux climatologies. *National Center for Atmospheric Research*

LARGE, W.G. and YEAGER, S.G. 2009. The global climatology of an interannually varying air-sea flux data set. *Climate Dynamics* 33: 341 – 364

LE BARS, D., DE RUIJTER, W.P.M, DIJKSTRA, H.A. 2012. A New Regime of the Agulhas Current Retroflection: Turbulent Choking of Indian-Atlantic leakage. *Journal of Physical Oceanography* 21: 1158 – 1172

LENTON, A. and MATEAR, R. 2007. Role of the Southern Annular Mode (SAM) in the Southern Ocean CO_2 uptake**.** *Global Biogeochemical Cycles* 21: 1 – 17

LIMPASUVAN, V. and HARTMANN, D.L. 1999. Eddies and the annular modes of climate variability. *Geophysical Research letters* 26(20): 3133 – 3136

LOVENDUSKI, N.S. and GRUBER, N. 2005. Impact of the Southern Annular Mode on Southern Ocean circulation and biology**.** *Geophysical Research Letters* 32(11)

LUTJEHARMS, J.R.E. 1985. Location of Frontal systems between Africa and Antarctica: some Preliminary Results. *Deep Sea Research Part I: Oceanographic Research Papers*. 32(12): 1499 – 1509

LUTJEHARMS, J.R.E. (2006). The Agulhas Current. Springer.

LUTJEHARMS, J.R.E. 2007. Three Decades of research on the greater Agulhas Current. *Ocean Science* 3(1): 129 – 147

LUJTEHARMS, J.R.E. and ANSORGE, I.J. 2001. The Agulhas Return Current. *Journal of Marine Systems* 30:115 – 138

LUTJEHARMS, J.R.E., BIASTOCH, A., VAN DER WERF, P.M., RIDDERINKHOF, H., DE RUIJTER, W.P.M. 2012. On the discontinuous nature of the Mozambique Current: research letter.

LUTJEHARMS, J.R.E., CATZEL, R., VALENTINE, H.R. 1989. Eddies and other boundary phenomena of the Agulhas Current. *Continental Shelf Research* 9(7): 597 – 616

LUTJEHARMS, J.R.E., MEYER, A.A., ANSORGE, I.J., EAGLE, G.A., ORREN, M.J. 1996. The nutrient characteristics of the Agulhas Bank. *South African Journal of Marine Science* 17: 253 – 274

LUTJEHARMS, J.R.E., VALENTINE, H.R. 1984. Southern Ocean thermal fronts south of Africa. *Deep Sea Research*. 31(12): 1461 – 1475

LUTJEHARMS, J.R.E. and VAN BALLEGOOYEN, R.C. 1984. Topographic control in the Agulhas Current system. *Deep Sea Research Part A. Oceanographic Research Papers* 31(11): 1321 – 1337

LUTJEHARMS, J.R.E. and VAN BALLEGOOYEN, R.C. 1988. The Retroflection of the Agulhas Current. *Journal of Physical Oceanography* 18: 1570 – 1583

LUTJEHARMS, J.R.E., WALTERS, N.M., ALLANSON, B.R. 1985. Oceanic Frontal Systems and Biological Enhancement. In *Antarctic Nutrient Cycles and Food Webs*. ed. SIEGFRIED, W.R., LAWS, R.M., CONDY, P.R. 11 – 31. Berlin: Springer Verlag

MARCHESIELLO, P., MCWILLIAMS, J.C., SHCHEPETKIN, A. 2001. Open boundary conditions for long-term integration of regional oceanic models. *Ocean Modelling* 3(1): 1 – 20

MARSHALL, G.J. 2003. Trends in the Southern Annular Mode from Observations and Reanalysis. *Journal of Climate* 16: 4134-4143

MOLINARI, R.L., MAYER, D.A., FESTA, J.F., BEZDEK, H.F. 1997. Multiyear variability in the near-surface temperature structure of the midlatitude western North Atlantic Ocean. *Journal of Geophysical Research* 102(C2): 3267 – 3278

OLSEN, D.B. and EVANS, R.H. 1986. Rings of the Agulhas Current. *Deep Sea Research*

Part A. Oceanographic Research Papers 33(1): 27 – 42

ORSI, A.H., WHITWORTH III, T., NOWLIN, W.D.Jr. 1995. On the meridional extent and the fronts of the Antarctic Circumpolar Current. *Deep-Sea Research I* 42(5): 641 – 673

PENVEN, P., MARCHESIELLO, P., DEBREU, L., LEFÈVRE, J. 2008. Software tools for pre- and post-processing of oceanic regional simulations. *Environmental Modelling and Software* 23(5): 660 – 662

PRICE, J.F., WELLER, R.A., SCHUDLICH, R.R. 1987. Wind-Driven Ocean Currents and Ekman Transport. *Science* 238: 1534 – 1538

RASMUSSON, E.M. and CARPENTER, T.H. 1982. Variations in Tropical Sea Surface Temperature and Surface Wind Fields associated with the Southern Oscillation/El Niño. *Monthly Weather Review* 110: 354 – 384

ROUAULT, M., PENVEN, P., POHL, B. 2009. Warming in the Agulhas Current system since the 1980's. *Geophysical Research Letters* 36(12)

ROUAULT, M., POHL, B., PENVEN, P. 2010. Coastal oceanic climate change and variability from 1982 to 2009 around South Africa. *African Journal of Marine Science* 32(2): 237 – 246

REASON, C.J.C., ALLEN, R.J., LINDESAY, J.A., ANSELL, T.J. 2000. ENSO and climatic signals across the Indian Ocean basin in the global context: Part I. Interannual composite patterns. *International Journal of Climatology* 20(11): 1285 – 1327

REASON, C.J.C., FLORENCHIE, P., ROUAULT, M., VEITCH, J. 2006. 10 Influences of large scale climate modes and agulhas system variability on the BCLME region. *Large*

Marine Ecosystems 14: 223 – 238

REASON, C.J.C. and MULENGA, H. 1999. Relationships between South African rainfall and SST anomalies in the southwest Indian Ocean. *International Journal of Climatology* 19(15): 1651 – 1673

REASON, C.J.C, and ROUAULT, M. 2002. ENSO-like decadal variability and the South African rainfall. *Geophysical Research Letters* 29(13): 1638

REASON, C.J.C. and ROUAULT, M. 2005. Links between the Antarctic Oscillation and winter rainfall over western South Africa. *Geophysical Research Letters* 32

ROGERS, J.C. and VAN LOON, H. 1982. Spatial Variability of Sea Level Pressure and 500 mb Height Anomalies over the Southern Hemisphere. *Monthly Weather Review* 110: 1375 – 1392

SHCHEPETKIN, A.F. and MCWILLIAMS, J.C. 2005. The regional oceanic modelling system (ROMS): a split-explicit, free-surface, topography-following-coordinate oceanic model. *Ocean Modelling* 9: 347 – 404

SILVESTRI, G.E. and VERA, C.S. 2003. Antarctic Oscillation signal on precipitation anomalies over southeastern South America. *Geaophysical Research Letters* 30(21)

SMITH, T.M., REYNOLDS, R.W., PETERSON, T.C., LAWRIMORE, J. 2008. Improvements to NOAA's Historical Merged Land-Ocean Surface Temperature Analysis (1880 – 2006). *Journal of Climate* 21(10): 2283 - 2296

SONG, Q., GORDON, A.L., VISBECK, M. 2004. Spreading of the Indonesian Throughflow in the Indian Ocean. *Journal of Physical Oceanography* 34: 772 – 792

STRAMMA, L. and LUTJEHARMS, J.R.E. 1997. The flow of the subtropical gyre of the South Indian Ocean. *Journal of Geophysical Research: Oceans* 102(C3): 5513 – 5530

TOURRE, Y.M. and WHITE, W.B. 2005. Evolution of the ENSO signal over the tropical Pacific-Atlantic domain. *Geophysical Research Letters* 32(7)

TRENBERTH, K.F. 1997. The Definition of El Niño**.** *Bulletin of the American Meteorological Society* 78: 2771 – 2777

TRENBERTH, K.E., and HOAR, T.J. 1997. El Nino and Climate Change. *Geophysical Research Letters* 24(23): 3057 – 3060

WALLACE, J., SMITH, C., BRETHERTON, C. 1992. Singular value decomposition of wintertime sea surface temperature and 500-mb height anomalies. *Journal of Climate* 5(6): 561 – 576

VAN LEEUWEN, P.J., DE RUIJTER, W.P.M., LUTJEHARMS, J.R.E. 2000. Natal pulses and the formation of Agulhas rings. *Journal of Geophysical Research: Oceans* 105(C3): 6425 – 6436

XUE, Y., SMITH, T.M., REYNOLDS, R.W. 2003. Interdecadal changes of the 30yr SST normal during 1871 – 2000. *Journal of Climate* 16: 1601 – 1612

ZHANG, R.H. and LEVITUS, S. 1996. Structure and evolution of interannual variability of the tropical Pacific upper ocean temperature. *Journal of Geophysical Research* 101(C9): 20501 – 20520

10. Index of Figures and Tables:

Figures:

Tables:

11. Appendix:

Appendix 11.1: ENSO Niño index from NOAA Climate Prediction Centre

Year	Month	TOTAL	Climate Adjusted	Anomalous index
1950	1	24.84	26.26	-1.42
1950	2	25.22	26.53	-1.31
1950	3	26.04	27.09	-1.04
1950	4	26.38	27.5	-1.12
1950	5	26.2	27.58	-1.38
1950	6	26.53	27.31	-0.78
1950	7	26.41	26.91	-0.5
1950	8	25.98	26.48	-0.5
1950	9	25.78	26.3	-0.52
1950	10	25.95	26.22	-0.27
1950	11	25.63	26.21	-0.59
1950	12	25.5	26.28	-0.78
1951	1	25.47	26.26	-0.79
1951	2	25.8	26.53	-0.73
1951	3	26.75	27.09	-0.34
1951	4	27.27	27.5	-0.24
1951	5	27.7	27.58	0.11
1951	6	27.46	27.31	0.15
1951	7	27.72	26.91	0.81
1951	8	27.34	26.48	0.86
1951	9	27.49	26.3	1.19
1951	10	27.42	26.22	1.2
1951	11	27.48	26.21	1.27
1951	12	27.13	26.28	0.85
1952	1	26.85	26.26	0.59
1952	2	26.8	26.53	0.27
1952	3	27.33	27.09	0.24
1952	4	27.88	27.5	0.38
1952	5	27.98	27.58	0.39
1952	6	27.32	27.31	0.01
1952	7	26.72	26.91	-0.19
1952	8	26.46	26.48	-0.02
1952	9	26.54	26.3	0.24
1952	10	26.53	26.22	0.31
1952	11	26.35	26.21	0.14
1952	12	26.53	26.28	0.25
1953	1	26.85	26.26	0.59
1953	2	27.19	26.53	0.66
1953	3	27.67	27.09	0.59
1953	4	28.19	27.5	0.68

1953	5	28.28	27.58	0.7
1953	6	28.02	27.31	0.71
1953	7	27.51	26.91	0.6
1953	8	27.15	26.48	0.66
1953	9	27.12	26.3	0.82
1953	10	27.02	26.22	0.8
1953	11	26.97	26.21	0.75
1953	12	27	26.28	0.72
1954	1	27.03	26.26	0.77
1954	2	27.22	26.53	0.69
1954	3	27.21	27.09	0.12
1954	4	26.86	27.5	-0.64
1954	5	27.06	27.58	-0.53
1954	6	26.92	27.31	-0.39
1954	7	26.36	26.91	-0.55
1954	8	25.73	26.48	-0.75
1954	9	25.37	26.3	-0.93
1954	10	25.5	26.22	-0.72
1954	11	25.66	26.21	-0.55
1954	12	25.37	26.28	-0.91
1955	1	25.55	26.26	-0.71
1955	2	25.91	26.53	-0.62
1955	3	26.38	27.09	-0.7
1955	4	26.67	27.5	-0.84
1955	5	26.66	27.58	-0.92
1955	6	26.55	27.31	-0.76
1955	7	26.3	26.91	-0.61
1955	8	25.6	26.48	-0.88
1955	9	25.61	26.3	-0.69
1955	10	24.66	26.22	-1.56
1955	11	24.29	26.21	-1.93
1955	12	24.59	26.28	-1.69
1956	1	25.29	26.4	-1.11
1956	2	26.01	26.64	-0.62
1956	3	26.64	27.15	-0.51
1956	4	26.98	27.57	-0.59
1956	5	27.23	27.61	-0.38
1956	6	26.98	27.37	-0.39
1956	7	26.37	26.97	-0.61
1956	8	25.9	26.52	-0.62
1956	9	25.89	26.33	-0.43
1956	10	25.83	26.26	-0.43
1956	11	25.64	26.25	-0.61

1956	12	25.71	26.29	-0.58
1957	1	26.1	26.4	-0.3
1957	2	26.59	26.64	-0.05
1957	3	27.64	27.15	0.49
1957	4	28.34	27.57	0.77
1957	5	28.57	27.61	0.96
1957	6	28.27	27.37	0.89
1957	7	28.1	26.97	1.13
1957	8	27.74	26.52	1.22
1957	9	27.53	26.33	1.2
1957	10	27.48	26.26	1.22
1957	11	27.79	26.25	1.54
1957	12	28.07	26.29	1.78
1958	1	28.36	26.4	1.96
1958	2	28.41	26.64	1.77
1958	3	28.33	27.15	1.18
1958	4	28.35	27.57	0.78
1958	5	28.34	27.61	0.72
1958	6	28.04	27.37	0.67
1958	7	27.47	26.97	0.49
1958	8	26.89	26.52	0.37
1958	9	26.49	26.33	0.16
1958	10	26.6	26.26	0.35
1958	11	26.89	26.25	0.64
1958	12	26.77	26.29	0.48
1959	1	27.13	26.4	0.73
1959	2	27.25	26.64	0.61
1959	3	27.55	27.15	0.4
1959	4	27.93	27.57	0.36
1959	5	27.8	27.61	0.19
1959	6	27.34	27.37	-0.04
1959	7	26.56	26.97	-0.42
1959	8	26.32	26.52	-0.2
1959	9	26.17	26.33	-0.16
1959	10	26.42	26.26	0.16
1959	11	26.32	26.25	0.07
1959	12	26.43	26.29	0.14
1960	1	26.25	26.4	-0.15
1960	2	26.28	26.64	-0.36
1960	3	26.97	27.15	-0.18
1960	4	27.51	27.57	-0.06
1960	5	27.61	27.61	0
1960	6	27.24	27.37	-0.14

1960	7	27.06	26.97	0.08
1960	8	26.84	26.52	0.32
1960	9	26.59	26.33	0.26
1960	10	26.34	26.26	0.08
1960	11	26.33	26.25	0.08
1960	12	26.4	26.29	0.11
1961	1	26.37	26.37	0.01
1961	2	26.61	26.6	0.01
1961	3	27	27.1	-0.1
1961	4	27.51	27.5	0.01
1961	5	27.85	27.55	0.3
1961	6	27.84	27.3	0.54
1961	7	27.13	26.92	0.21
1961	8	26.41	26.49	-0.09
1961	9	25.96	26.34	-0.38
1961	10	25.93	26.27	-0.34
1961	11	26.2	26.24	-0.04
1961	12	26.2	26.27	-0.07
1962	1	26.12	26.37	-0.24
1962	2	26.29	26.6	-0.31
1962	3	26.8	27.1	-0.29
1962	4	27.23	27.5	-0.27
1962	5	27.23	27.55	-0.32
1962	6	27.17	27.3	-0.12
1962	7	26.92	26.92	0
1962	8	26.51	26.49	0.01
1962	9	26.07	26.34	-0.27
1962	10	26.05	26.27	-0.22
1962	11	25.88	26.24	-0.36
1962	12	25.75	26.27	-0.52
1963	1	25.87	26.37	-0.5
1963	2	26.39	26.6	-0.21
1963	3	27.31	27.1	0.21
1963	4	27.87	27.5	0.37
1963	5	27.7	27.55	0.16
1963	6	27.68	27.3	0.38
1963	7	27.89	26.92	0.97
1963	8	27.62	26.49	1.13
1963	9	27.45	26.34	1.11
1963	10	27.55	26.27	1.28
1963	11	27.6	26.24	1.36
1963	12	27.7	26.27	1.43
1964	1	27.42	26.37	1.05

1964	2	27.27	26.6	0.67
1964	3	27.11	27.1	0.01
1964	4	27.06	27.5	-0.44
1964	5	26.93	27.55	-0.61
1964	6	26.65	27.3	-0.64
1964	7	26.41	26.92	-0.51
1964	8	25.73	26.49	-0.76
1964	9	25.48	26.34	-0.86
1964	10	25.53	26.27	-0.74
1964	11	25.4	26.24	-0.84
1964	12	25.41	26.27	-0.86
1965	1	25.78	26.37	-0.58
1965	2	26.37	26.6	-0.23
1965	3	27.13	27.1	0.03
1965	4	27.62	27.5	0.12
1965	5	28.07	27.55	0.52
1965	6	28.19	27.3	0.89
1965	7	28.01	26.92	1.09
1965	8	28.06	26.49	1.57
1965	9	28.02	26.34	1.68
1965	10	28.24	26.27	1.97
1965	11	28.28	26.24	2.04
1965	12	28.05	26.27	1.79
1966	1	27.74	26.46	1.29
1966	2	27.66	26.67	0.99
1966	3	28.21	27.14	1.07
1966	4	28.24	27.5	0.74
1966	5	27.67	27.61	0.06
1966	6	27.77	27.42	0.35
1966	7	27.41	27.04	0.37
1966	8	26.65	26.62	0.03
1966	9	26.48	26.51	-0.04
1966	10	26.4	26.49	-0.09
1966	11	26.41	26.49	-0.08
1966	12	26.2	26.45	-0.25
1967	1	26.17	26.46	-0.29
1967	2	26.36	26.67	-0.31
1967	3	26.67	27.14	-0.47
1967	4	26.92	27.5	-0.58
1967	5	27.5	27.61	-0.11
1967	6	27.61	27.42	0.2
1967	7	27.16	27.04	0.12
1967	8	26.6	26.62	-0.02

1967	9	26.09	26.51	-0.43
1967	10	26.18	26.49	-0.31
1967	11	26.25	26.49	-0.24
1967	12	26.09	26.45	-0.36
1968	1	25.78	26.46	-0.68
1968	2	25.79	26.67	-0.87
1968	3	26.38	27.14	-0.76
1968	4	27.09	27.5	-0.41
1968	5	27.16	27.61	-0.45
1968	6	27.69	27.42	0.27
1968	7	27.6	27.04	0.56
1968	8	27.11	26.62	0.49
1968	9	26.89	26.51	0.37
1968	10	26.98	26.49	0.49
1968	11	27.37	26.49	0.88
1968	12	27.42	26.45	0.97
1969	1	27.55	26.46	1.09
1969	2	27.95	26.67	1.29
1969	3	28.02	27.14	0.88
1969	4	28.39	27.5	0.89
1969	5	28.5	27.61	0.89
1969	6	28	27.42	0.58
1969	7	27.3	27.04	0.26
1969	8	27.16	26.62	0.54
1969	9	27.33	26.51	0.82
1969	10	27.5	26.49	1.01
1969	11	27.35	26.49	0.86
1969	12	27.31	26.45	0.86
1970	1	27.07	26.46	0.61
1970	2	27.04	26.67	0.38
1970	3	27.37	27.14	0.23
1970	4	27.96	27.5	0.45
1970	5	27.77	27.61	0.16
1970	6	27.13	27.42	-0.29
1970	7	26.47	27.04	-0.57
1970	8	25.86	26.62	-0.76
1970	9	25.86	26.51	-0.66
1970	10	25.78	26.49	-0.71
1970	11	25.82	26.49	-0.67
1970	12	25.47	26.45	-0.98
1971	1	25.1	26.52	-1.42
1971	2	25.41	26.72	-1.31
1971	3	26.11	27.18	-1.07

1971	4	26.79	27.55	-0.76
1971	5	27.06	27.65	-0.59
1971	6	26.7	27.47	-0.77
1971	7	26.29	27.05	-0.77
1971	8	25.97	26.66	-0.69
1971	9	25.93	26.56	-0.63
1971	10	25.64	26.56	-0.92
1971	11	25.69	26.55	-0.87
1971	12	25.55	26.52	-0.97
1972	1	25.85	26.52	-0.67
1972	2	26.43	26.72	-0.28
1972	3	27.22	27.18	0.04
1972	4	27.94	27.55	0.39
1972	5	28.27	27.65	0.62
1972	6	28.23	27.47	0.77
1972	7	28.18	27.05	1.13
1972	8	28.1	26.66	1.44
1972	9	28.09	26.56	1.54
1972	10	28.45	26.56	1.89
1972	11	28.68	26.55	2.13
1972	12	28.8	26.52	2.27
1973	1	28.43	26.52	1.91
1973	2	27.99	26.72	1.28
1973	3	27.72	27.18	0.54
1973	4	27.39	27.55	-0.16
1973	5	27.13	27.65	-0.53
1973	6	26.74	27.47	-0.73
1973	7	25.95	27.05	-1.11
1973	8	25.46	26.66	-1.2
1973	9	25.32	26.56	-1.24
1973	10	25.04	26.56	-1.52
1973	11	24.51	26.55	-2.05
1973	12	24.44	26.52	-2.08
1974	1	24.53	26.52	-1.99
1974	2	25.14	26.72	-1.57
1974	3	25.93	27.18	-1.24
1974	4	26.65	27.55	-0.9
1974	5	26.86	27.65	-0.8
1974	6	26.72	27.47	-0.75
1974	7	26.48	27.05	-0.57
1974	8	26.36	26.66	-0.3
1974	9	26.22	26.56	-0.34
1974	10	25.91	26.56	-0.65

1974	11	25.63	26.55	-0.92
1974	12	25.7	26.52	-0.82
1975	1	26.19	26.52	-0.33
1975	2	26.24	26.72	-0.48
1975	3	26.46	27.18	-0.72
1975	4	27.01	27.55	-0.54
1975	5	26.97	27.65	-0.68
1975	6	26.3	27.47	-1.17
1975	7	25.98	27.05	-1.07
1975	8	25.47	26.66	-1.19
1975	9	25.2	26.56	-1.36
1975	10	24.87	26.56	-1.69
1975	11	25.1	26.55	-1.45
1975	12	24.76	26.52	-1.76
1976	1	24.73	26.5	-1.78
1976	2	25.59	26.69	-1.1
1976	3	26.61	27.16	-0.55
1976	4	27	27.54	-0.53
1976	5	27.28	27.62	-0.33
1976	6	27.35	27.45	-0.1
1976	7	27.26	27.06	0.2
1976	8	27.09	26.7	0.39
1976	9	27.12	26.63	0.49
1976	10	27.48	26.6	0.88
1976	11	27.42	26.57	0.85
1976	12	27.16	26.53	0.63
1977	1	27.32	26.5	0.81
1977	2	27.16	26.69	0.47
1977	3	27.58	27.16	0.43
1977	4	27.61	27.54	0.08
1977	5	27.96	27.62	0.34
1977	6	27.95	27.45	0.5
1977	7	27.55	27.06	0.49
1977	8	26.92	26.7	0.22
1977	9	27.2	26.63	0.57
1977	10	27.36	26.6	0.76
1977	11	27.28	26.57	0.7
1977	12	27.36	26.53	0.83
1978	1	27.32	26.5	0.81
1978	2	27.17	26.69	0.48
1978	3	27.24	27.16	0.09
1978	4	27.26	27.54	-0.28
1978	5	27.35	27.62	-0.26

1978	6	27.16	27.45	-0.29
1978	7	26.8	27.06	-0.26
1978	8	26.23	26.7	-0.47
1978	9	26.2	26.63	-0.43
1978	10	26.4	26.6	-0.19
1978	11	26.43	26.57	-0.14
1978	12	26.49	26.53	-0.04
1979	1	26.45	26.5	-0.05
1979	2	26.62	26.69	-0.07
1979	3	27.48	27.16	0.33
1979	4	27.87	27.54	0.33
1979	5	27.75	27.62	0.13
1979	6	27.55	27.45	0.1
1979	7	26.96	27.06	-0.1
1979	8	26.77	26.7	0.07
1979	9	27.15	26.63	0.52
1979	10	27.01	26.6	0.41
1979	11	27.08	26.57	0.51
1979	12	27.09	26.53	0.56
1980	1	27.1	26.5	0.59
1980	2	27.03	26.69	0.34
1980	3	27.38	27.16	0.23
1980	4	27.78	27.54	0.25
1980	5	27.98	27.62	0.37
1980	6	27.99	27.45	0.54
1980	7	27.35	27.06	0.29
1980	8	26.62	26.7	-0.08
1980	9	26.57	26.63	-0.06
1980	10	26.51	26.6	-0.09
1980	11	26.63	26.57	0.06
1980	12	26.59	26.53	0.06
1981	1	26.18	26.68	-0.5
1981	2	26.15	26.84	-0.69
1981	3	26.77	27.29	-0.52
1981	4	27.33	27.69	-0.36
1981	5	27.41	27.77	-0.35
1981	6	27.35	27.56	-0.21
1981	7	26.67	27.12	-0.46
1981	8	26.25	26.74	-0.49
1981	9	26.53	26.69	-0.16
1981	10	26.52	26.64	-0.12
1981	11	26.41	26.63	-0.22
1981	12	26.48	26.62	-0.14

1982	1	26.7	26.68	0.02
1982	2	26.73	26.84	-0.11
1982	3	27.36	27.29	0.08
1982	4	27.91	27.69	0.22
1982	5	28.42	27.77	0.65
1982	6	28.32	27.56	0.76
1982	7	27.65	27.12	0.52
1982	8	27.64	26.74	0.9
1982	9	28.2	26.69	1.51
1982	10	28.67	26.64	2.03
1982	11	28.71	26.63	2.07
1982	12	28.93	26.62	2.31
1983	1	28.92	26.68	2.25
1983	2	28.74	26.84	1.9
1983	3	28.76	27.29	1.47
1983	4	28.74	27.69	1.05
1983	5	28.83	27.77	1.06
1983	6	28.27	27.56	0.72
1983	7	27.19	27.12	0.07
1983	8	26.53	26.74	-0.21
1983	9	26.19	26.69	-0.5
1983	10	25.76	26.64	-0.89
1983	11	25.55	26.63	-1.09
1983	12	25.82	26.62	-0.8
1984	1	26.14	26.68	-0.54
1984	2	26.72	26.84	-0.12
1984	3	27.05	27.29	-0.23
1984	4	27.3	27.69	-0.39
1984	5	27.3	27.77	-0.46
1984	6	26.95	27.56	-0.61
1984	7	26.84	27.12	-0.29
1984	8	26.66	26.74	-0.08
1984	9	26.43	26.69	-0.26
1984	10	26.15	26.64	-0.5
1984	11	25.61	26.63	-1.02
1984	12	25.38	26.62	-1.23
1985	1	25.58	26.68	-1.09
1985	2	26.12	26.84	-0.72
1985	3	26.54	27.29	-0.75
1985	4	26.93	27.69	-0.76
1985	5	27.09	27.77	-0.68
1985	6	26.92	27.56	-0.64
1985	7	26.63	27.12	-0.49

1985	8	26.27	26.74	-0.47
1985	9	26.08	26.69	-0.61
1985	10	26.22	26.64	-0.43
1985	11	26.38	26.63	-0.26
1985	12	26.19	26.62	-0.43
1986	1	26.04	26.56	-0.52
1986	2	26.28	26.75	-0.47
1986	3	27.01	27.24	-0.23
1986	4	27.65	27.67	-0.02
1986	5	27.58	27.78	-0.2
1986	6	27.56	27.53	0.03
1986	7	27.38	27.11	0.28
1986	8	27.21	26.75	0.46
1986	9	27.35	26.7	0.65
1986	10	27.59	26.64	0.95
1986	11	27.67	26.6	1.07
1986	12	27.74	26.57	1.17
1987	1	27.81	26.56	1.25
1987	2	28.03	26.75	1.28
1987	3	28.5	27.24	1.26
1987	4	28.69	27.67	1.02
1987	5	28.7	27.78	0.93
1987	6	28.66	27.53	1.13
1987	7	28.51	27.11	1.41
1987	8	28.47	26.75	1.72
1987	9	28.41	26.7	1.71
1987	10	28.07	26.64	1.43
1987	11	27.93	26.6	1.33
1987	12	27.6	26.57	1.03
1988	1	27.5	26.56	0.94
1988	2	27.02	26.75	0.28
1988	3	27.46	27.24	0.22
1988	4	27.57	27.67	-0.1
1988	5	26.97	27.78	-0.81
1988	6	26.2	27.53	-1.33
1988	7	25.66	27.11	-1.45
1988	8	25.71	26.75	-1.04
1988	9	25.72	26.7	-0.98
1988	10	24.83	26.64	-1.81
1988	11	24.74	26.6	-1.87
1988	12	24.68	26.57	-1.89
1989	1	24.71	26.56	-1.85
1989	2	25.35	26.75	-1.39

1989	3	26.13	27.24	-1.11
1989	4	26.85	27.67	-0.83
1989	5	27.19	27.78	-0.59
1989	6	27.24	27.53	-0.29
1989	7	26.79	27.11	-0.31
1989	8	26.42	26.75	-0.33
1989	9	26.46	26.7	-0.24
1989	10	26.31	26.64	-0.33
1989	11	26.28	26.6	-0.32
1989	12	26.58	26.57	0.01
1990	1	26.63	26.56	0.07
1990	2	27.04	26.75	0.3
1990	3	27.41	27.24	0.16
1990	4	27.95	27.67	0.28
1990	5	28.08	27.78	0.3
1990	6	27.63	27.53	0.1
1990	7	27.42	27.11	0.32
1990	8	27.16	26.75	0.41
1990	9	26.96	26.7	0.26
1990	10	27.01	26.64	0.37
1990	11	26.88	26.6	0.28
1990	12	26.97	26.57	0.4
1991	1	27.08	26.7	0.37
1991	2	27.13	26.87	0.26
1991	3	27.39	27.37	0.02
1991	4	28.11	27.78	0.33
1991	5	28.36	27.9	0.47
1991	6	28.41	27.69	0.71
1991	7	28.17	27.29	0.88
1991	8	27.72	26.93	0.79
1991	9	27.41	26.88	0.53
1991	10	27.61	26.85	0.76
1991	11	27.92	26.79	1.13
1991	12	28.3	26.75	1.55
1992	1	28.35	26.7	1.65
1992	2	28.42	26.87	1.55
1992	3	28.65	27.37	1.28
1992	4	29.05	27.78	1.27
1992	5	29.01	27.9	1.12
1992	6	28.35	27.69	0.66
1992	7	27.56	27.29	0.27
1992	8	26.97	26.93	0.04
1992	9	26.67	26.88	-0.21

1992	10	26.4	26.85	-0.45
1992	11	26.59	26.79	-0.2
1992	12	26.71	26.75	-0.04
1993	1	26.88	26.7	0.17
1993	2	27.21	26.87	0.34
1993	3	27.72	27.37	0.35
1993	4	28.5	27.78	0.72
1993	5	28.7	27.9	0.81
1993	6	28.08	27.69	0.38
1993	7	27.6	27.29	0.31
1993	8	27.02	26.93	0.09
1993	9	27.14	26.88	0.27
1993	10	27.01	26.85	0.16
1993	11	26.92	26.79	0.13
1993	12	26.79	26.75	0.04
1994	1	26.75	26.7	0.05
1994	2	26.97	26.87	0.1
1994	3	27.52	27.37	0.15
1994	4	28.12	27.78	0.33
1994	5	28.27	27.9	0.37
1994	6	28.09	27.69	0.4
1994	7	27.67	27.29	0.38
1994	8	27.39	26.93	0.46
1994	9	27.25	26.88	0.37
1994	10	27.54	26.85	0.69
1994	11	27.95	26.79	1.16
1994	12	28.01	26.75	1.26
1995	1	27.74	26.7	1.04
1995	2	27.68	26.87	0.81
1995	3	27.92	27.37	0.55
1995	4	28.17	27.78	0.38
1995	5	27.87	27.9	-0.02
1995	6	27.8	27.69	0.11
1995	7	27.25	27.29	-0.04
1995	8	26.42	26.93	-0.51
1995	9	26.2	26.88	-0.68
1995	10	26.08	26.85	-0.77
1995	11	25.83	26.79	-0.96
1995	12	25.87	26.75	-0.88
1996	1	25.85	26.68	-0.83
1996	2	25.99	26.84	-0.84
1996	3	26.75	27.34	-0.59
1996	4	27.42	27.8	-0.38

1996	5	27.65	27.91	-0.27
1996	6	27.49	27.69	-0.2
1996	7	27.01	27.28	-0.27
1996	8	26.75	26.93	-0.18
1996	9	26.44	26.82	-0.39
1996	10	26.49	26.79	-0.3
1996	11	26.43	26.74	-0.3
1996	12	26.13	26.69	-0.56
1997	1	26.09	26.68	-0.58
1997	2	26.47	26.84	-0.37
1997	3	27.15	27.34	-0.19
1997	4	27.98	27.8	0.18
1997	5	28.63	27.91	0.71
1997	6	28.86	27.69	1.17
1997	7	28.86	27.28	1.58
1997	8	28.69	26.93	1.76
1997	9	28.89	26.82	2.06
1997	10	29.13	26.79	2.35
1997	11	29.12	26.74	2.39
1997	12	29.04	26.69	2.35
1998	1	28.98	26.68	2.3
1998	2	28.72	26.84	1.88
1998	3	28.67	27.34	1.33
1998	4	28.66	27.8	0.85
1998	5	28.48	27.91	0.56
1998	6	27.42	27.69	-0.27
1998	7	26.53	27.28	-0.75
1998	8	25.93	26.93	-1
1998	9	25.66	26.82	-1.17
1998	10	25.46	26.79	-1.33
1998	11	25.49	26.74	-1.25
1998	12	25.13	26.69	-1.56
1999	1	24.97	26.68	-1.7
1999	2	25.59	26.84	-1.25
1999	3	26.45	27.34	-0.89
1999	4	26.93	27.8	-0.87
1999	5	27	27.91	-0.91
1999	6	26.67	27.69	-1.02
1999	7	26.28	27.28	-1
1999	8	25.82	26.93	-1.11
1999	9	25.76	26.82	-1.06
1999	10	25.61	26.79	-1.17
1999	11	25.21	26.74	-1.53

1999	12	24.97	26.69	-1.72
2000	1	24.89	26.68	-1.79
2000	2	25.25	26.84	-1.59
2000	3	26.29	27.34	-1.05
2000	4	27	27.8	-0.8
2000	5	27.11	27.91	-0.81
2000	6	26.97	27.69	-0.72
2000	7	26.69	27.28	-0.58
2000	8	26.46	26.93	-0.47
2000	9	26.32	26.82	-0.5
2000	10	26.12	26.79	-0.67
2000	11	26.01	26.74	-0.73
2000	12	25.83	26.69	-0.86
2001	1	25.94	26.68	-0.74
2001	2	26.26	26.84	-0.58
2001	3	26.9	27.34	-0.43
2001	4	27.4	27.8	-0.41
2001	5	27.71	27.91	-0.21
2001	6	27.61	27.69	-0.08
2001	7	27.37	27.28	0.09
2001	8	26.95	26.93	0.02
2001	9	26.74	26.82	-0.08
2001	10	26.66	26.79	-0.12
2001	11	26.47	26.74	-0.26
2001	12	26.33	26.69	-0.36
2002	1	26.5	26.68	-0.18
2002	2	26.84	26.84	0
2002	3	27.5	27.34	0.16
2002	4	28.01	27.8	0.21
2002	5	28.44	27.91	0.52
2002	6	28.48	27.69	0.79
2002	7	28.03	27.28	0.75
2002	8	27.66	26.93	0.73
2002	9	27.74	26.82	0.92
2002	10	27.94	26.79	1.15
2002	11	28.13	26.74	1.4
2002	12	28.08	26.69	1.39
2003	1	27.69	26.68	1.01
2003	2	27.63	26.84	0.79
2003	3	27.85	27.34	0.51
2003	4	27.75	27.8	-0.05
2003	5	27.42	27.91	-0.49
2003	6	27.56	27.69	-0.13

2003	7	27.66	27.28	0.38
2003	8	27.33	26.93	0.4
2003	9	27.1	26.82	0.28
2003	10	27.33	26.79	0.54
2003	11	27.14	26.74	0.4
2003	12	27.06	26.69	0.37
2004	1	26.92	26.68	0.24
2004	2	27.06	26.84	0.22
2004	3	27.4	27.34	0.06
2004	4	27.92	27.8	0.11
2004	5	28.01	27.91	0.1
2004	6	27.93	27.69	0.24
2004	7	27.85	27.28	0.57
2004	8	27.66	26.93	0.73
2004	9	27.57	26.82	0.75
2004	10	27.53	26.79	0.75
2004	11	27.38	26.74	0.64
2004	12	27.38	26.69	0.69
2005	1	27.32	26.68	0.64
2005	2	27.18	26.84	0.34
2005	3	27.64	27.34	0.3
2005	4	28.03	27.8	0.23
2005	5	28.3	27.91	0.39
2005	6	28	27.69	0.31
2005	7	27.45	27.28	0.17
2005	8	27.11	26.93	0.18
2005	9	26.79	26.82	-0.03
2005	10	26.71	26.79	-0.08
2005	11	26.12	26.74	-0.62
2005	12	25.79	26.69	-0.9
2006	1	25.69	26.68	-0.99
2006	2	26.16	26.84	-0.68
2006	3	26.81	27.34	-0.53
2006	4	27.54	27.8	-0.26
2006	5	27.91	27.91	0
2006	6	27.82	27.69	0.13
2006	7	27.36	27.28	0.09
2006	8	27.26	26.93	0.33
2006	9	27.33	26.82	0.5
2006	10	27.48	26.79	0.7
2006	11	27.82	26.74	1.08
2006	12	27.87	26.69	1.18
2007	1	27.37	26.68	0.7

2007	2	26.99	26.84	0.15
2007	3	27.26	27.34	-0.07
2007	4	27.57	27.8	-0.23
2007	5	27.54	27.91	-0.37
2007	6	27.54	27.69	-0.15
2007	7	26.99	27.28	-0.29
2007	8	26.4	26.93	-0.53
2007	9	25.86	26.82	-0.97
2007	10	25.72	26.79	-1.06
2007	11	25.47	26.74	-1.26
2007	12	25.41	26.69	-1.28
2008	1	25.07	26.68	-1.6
2008	2	25.2	26.84	-1.63
2008	3	26.18	27.34	-1.16
2008	4	26.98	27.8	-0.82
2008	5	27.2	27.91	-0.71
2008	6	27.15	27.69	-0.54
2008	7	27	27.28	-0.28
2008	8	26.81	26.93	-0.12
2008	9	26.7	26.82	-0.12
2008	10	26.67	26.79	-0.12
2008	11	26.52	26.74	-0.21
2008	12	25.78	26.69	-0.91
2009	1	25.7	26.68	-0.98
2009	2	26.04	26.84	-0.8
2009	3	26.67	27.34	-0.67
2009	4	27.54	27.8	-0.26
2009	5	28.11	27.91	0.19
2009	6	28.06	27.69	0.37
2009	7	27.88	27.28	0.6
2009	8	27.51	26.93	0.58
2009	9	27.48	26.82	0.65
2009	10	27.73	26.79	0.95
2009	11	28.17	26.74	1.43
2009	12	28.5	26.69	1.82
2010	1	28.31	26.68	1.63
2010	2	28.19	26.84	1.35
2010	3	28.46	27.34	1.13
2010	4	28.49	27.8	0.69
2010	5	28.13	27.91	0.21
2010	6	27.35	27.69	-0.34
2010	7	26.44	27.28	-0.84
2010	8	25.71	26.93	-1.22

2010	9	25.36	26.82	-1.46
2010	10	25.25	26.79	-1.54
2010	11	25.2	26.74	-1.54
2010	12	25.3	26.69	-1.39
2011	1	25.13	26.68	-1.54
2011	2	25.55	26.84	-1.29
2011	3	26.34	27.34	-1
2011	4	27.13	27.8	-0.67
2011	5	27.54	27.91	-0.37
2011	6	27.61	27.69	-0.08
2011	7	27.24	27.28	-0.04
2011	8	26.57	26.93	-0.36
2011	9	26.22	26.82	-0.61
2011	10	25.97	26.79	-0.81
2011	11	25.75	26.74	-0.99
2011	12	25.61	26.69	-1.08
2012	1	25.77	26.68	-0.91
2012	2	26.16	26.84	-0.68
2012	3	26.93	27.34	-0.41
2012	4	27.48	27.8	-0.32
2012	5	27.74	27.91	-0.18
2012	6	27.79	27.69	0.1
2012	7	27.26	27.28	-0.02
2012	8	27.12	26.93	0.19
2012	9	27.42	26.82	0.6
2012	10	27.25	26.79	0.46
2012	11	27.57	26.74	0.83
2012	12	26.6	26.69	-0.09

Appendix 11.2: SODA SSH Plots

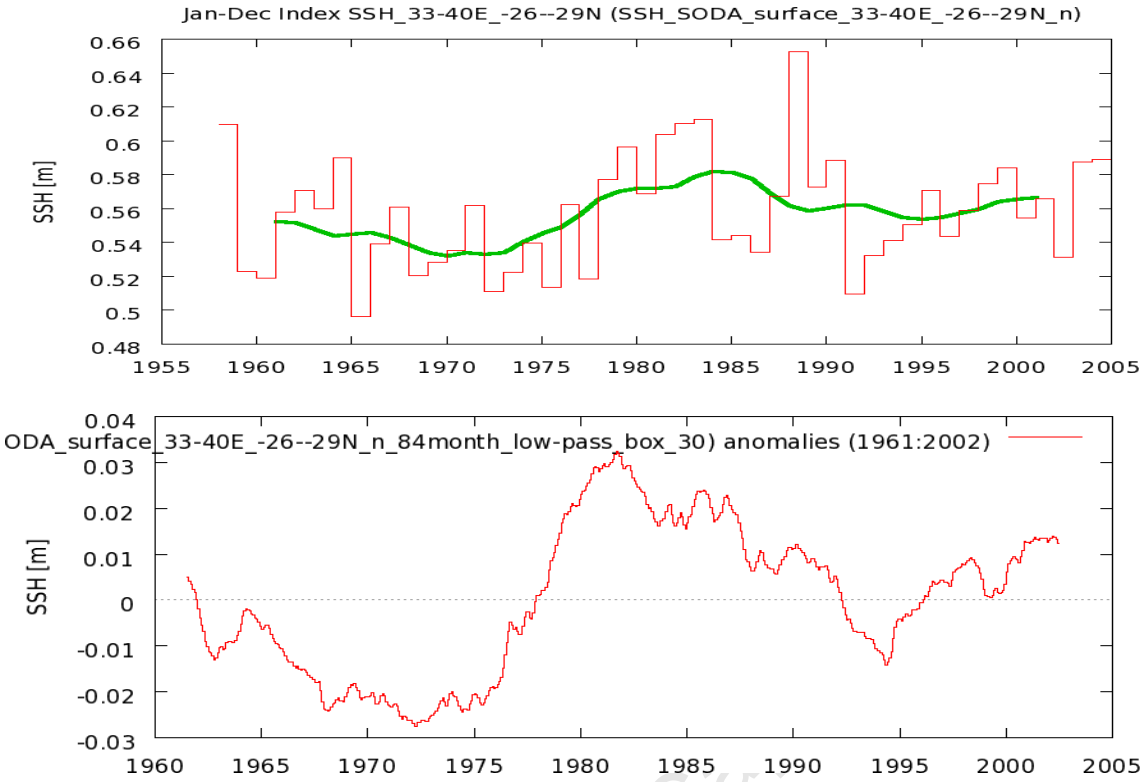

Figure 11.2.1: North Agulhas SSH, annual and anomalies with 7 year running mean respectively

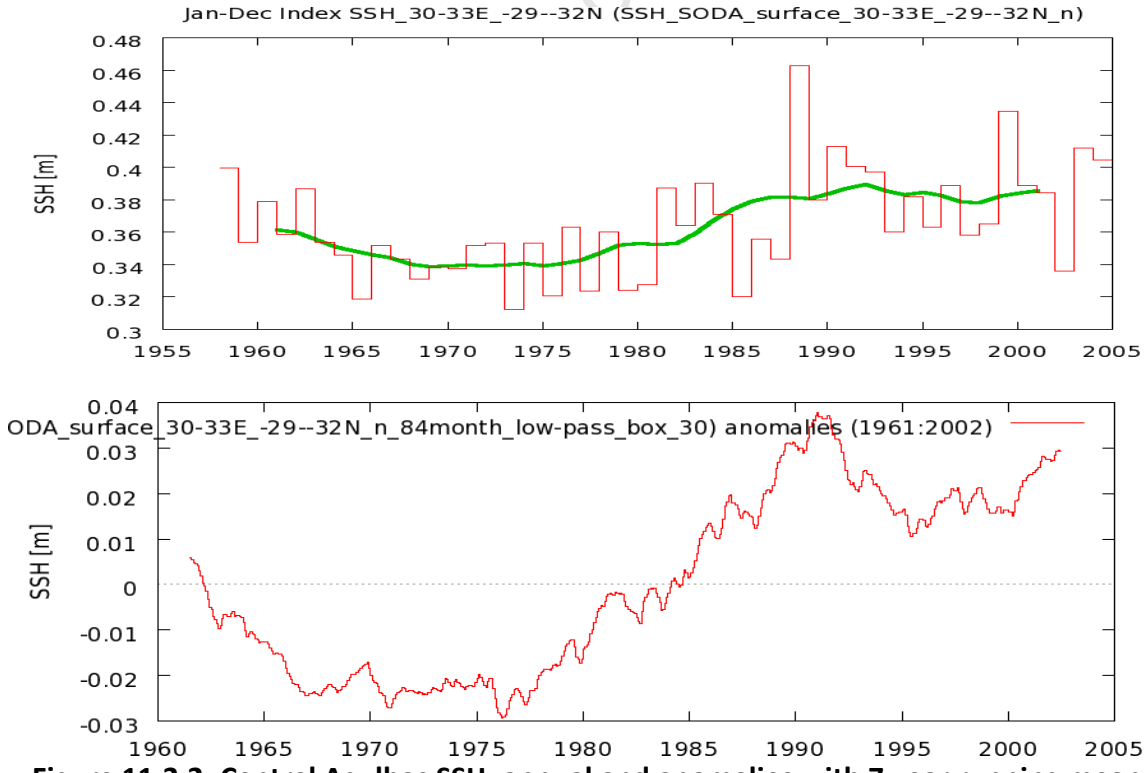

Figure 11.2.2: Central Agulhas SSH, annual and anomalies with 7 year running mean respectively

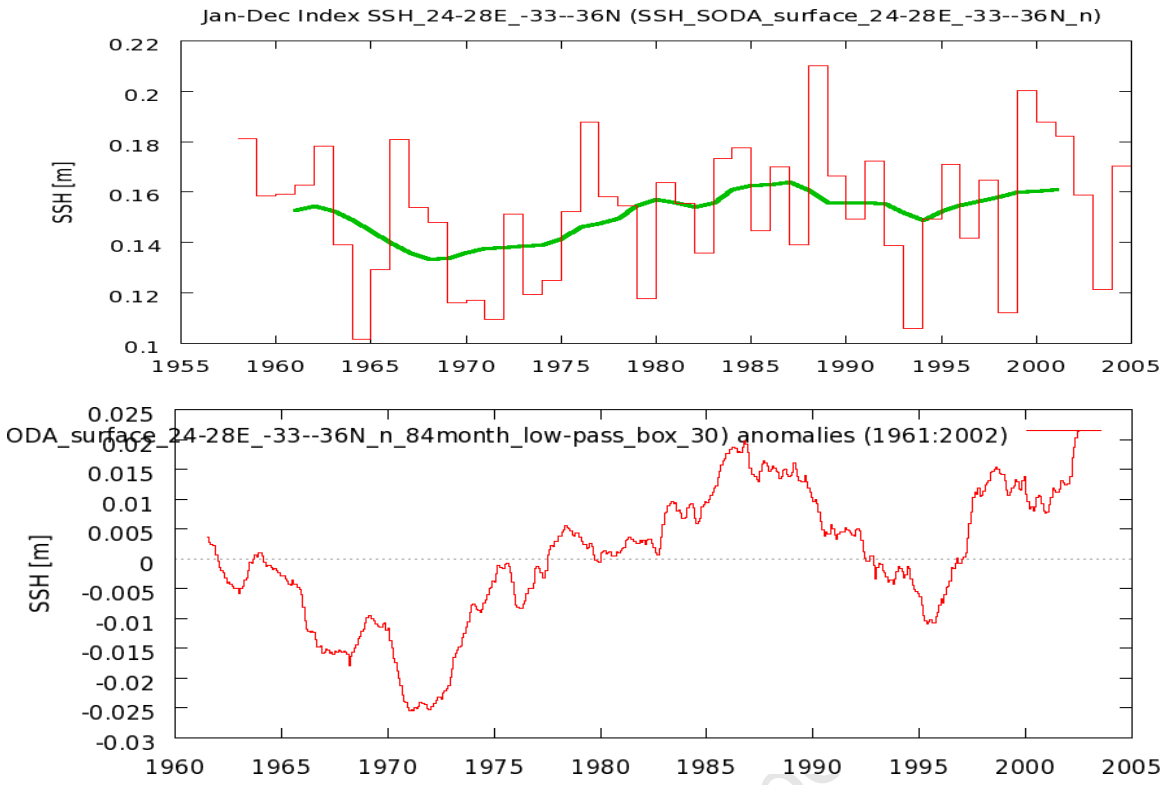

Figure 11.2.3: South Agulhas SSH, annual and anomalies with 7 year running mean respectively

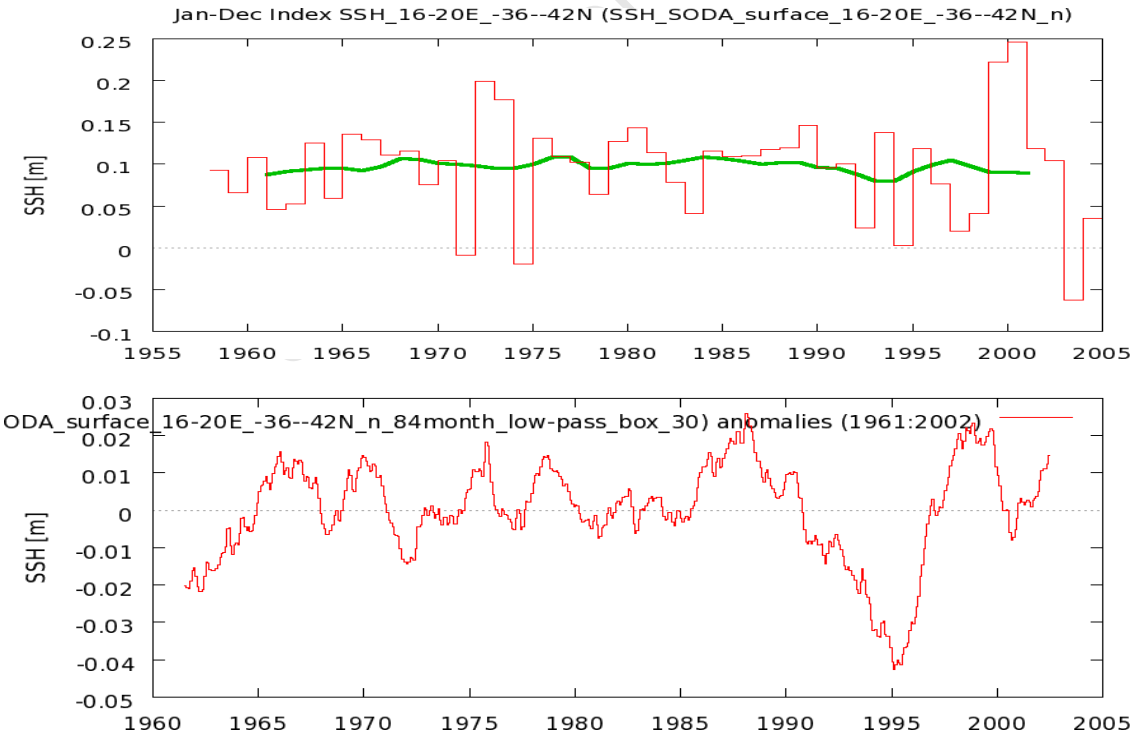

Figure 11.2.4: Retroflection SSH, annual and anomalies with 7 year running mean respectively

Appendix 11.3: Modelled SSH results on reduced time-series

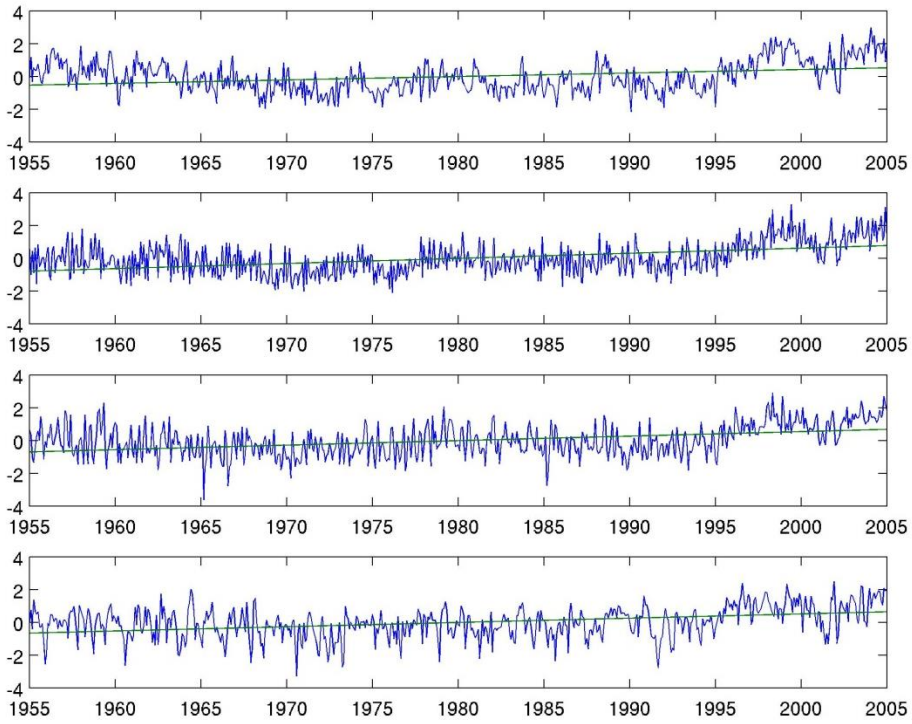

Figure 11.3.1: Anomalous SSH for 1955 to 2005 for the Northern Agulhas, Central Agulhas, Southern Agulhas and Retroflection blocks respectively

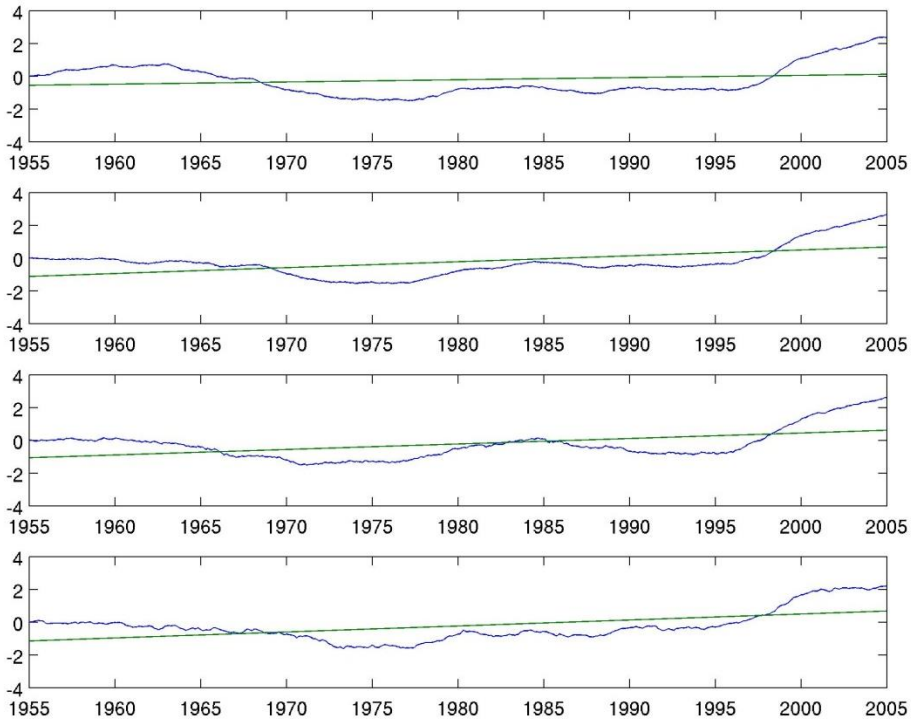

Figure 11.3.2: Anomalous SSH for 1955 to 2005 smoothed with a 7 year running mean for the Northern Agulhas, Central Agulhas and Retroflection blocks respectively